

JUNCTION STUDIES BETWEEN ALUMINUM
AND POLYMER, POLY[2-METHOXY-5-(3',7'-
DIMETHYLOCTYLOXY)-1, 4-PHENYLENE
VINYLENE], MDMO-PPV AND MDMO-PPV
BLENDED WITH C_{60}

A Thesis Submitted to the
School of Graduate studies
of Addis Ababa University



In Partial Fulfilment of the
Requirement for the Degree of
Master of Science in physics

Submitted by

Zelalem Nigussa

Addis Ababa, Ethiopia

June 2005

This work is dedicated to

my father: Nigussa Urgessa

and

my mother: Alemi Emirie

DECLARATION

I hereby declare that this thesis is my original work and has not been presented for a degree in any other University. All sources of material used for the thesis have been duly acknowledged.

Name: Zelalem Nigussa

Signature: _____

email: zolahan2005@yahoo.com

Place and date of submission: Addis Ababa University, June 2005

This Thesis has been submitted for examination with my approval as University advisor:

Name: Dr. Genene Tesema.

Signature: _____

ADDIS ABABA UNIVERSITY
SCHOOL OF GRADUATE STUDIES

JUNCTION STUDIES BETWEEN ALUMINUM AND POLYMER,
POLY[2-METHOXY-5-(3',7'-DIMETHYLOCTYLOXY)-1, 4-PHENYLENE
VINYLENE], MDMO-PPV AND MDMO-PPV BLENDED WITH C_{60}

BY

Zelalem Nigussa
Department of Physics
Faculty of Science

APPROVED BY THE EXAMINATION COMMITTEE

Name

Signature

Dr. Genene Tesema , _____, **Advisor**

Dr. L.L Henry, _____, **External Examiner**

Dr. Mebiratu G/Meriam, _____, **Internal Examiner**

Acknowledgment

I offer my deepest gratitude and special affection first and foremost to my advisor, Dr. Genene Tesema, for introducing me to the field of conjugated polymer and for his unlimited, excellent guidance, encouragement followed by suggestion and comments. The convenient working environment he has allowed me specially, the availability of easy, powerful and sophisticated softwares he has created for measurement and in writing this paper is greatly appreciated and encouraged. It is great privilege to work with him.

Special thanks are due to Dr. Teketel Yohannes, from the Department of Chemistry, for the material support and valuable comments on data collection phase of this work. The discussions with him always brought up interesting ideas for new studies and possible interpretations of the observed data. I would like to express my sincere thanks to Mr. Ushula Mengesha, a graduate student in the department of Physical chemistry and Mr. Assefa Sergawie, a Ph.D student in the same department working on conducting polymer, who gave me fruit full suggestion during the whole work especially in the material preparation. I am indebted to my colleague Mr. Teshome Sanbata for his unmeasurable help during the whole work both emotionally and physically. I also appreciate his patience in all aspects.

I would like to express my sincere thanks to my father, mother, sisters and brothers for their encouragement. I thank the Physics Department community and my instructors in the department for their help in one way or another for my success.

Last, but not least, Alemaya University (AU) is acknowledged for sponsoring me to join the School of Graduate Study.

Addis Ababa, Ethiopia

Zelalem Nigussa

Jun, 2005

Contents

Acknowledgment	i
List of Tables	iv
List of Figures	v
Abstract	x
Introduction	1
Chapter 1	5
1 Chemical bonding and physics of conjugated polymers	5
1.1 Molecular structure	5
1.1.1 σ and π -bonds	5
1.1.2 Hybridization	7
1.1.2.1 sp^3 Hybridization	8
1.1.2.2 sp^2 Hybridization	9
1.2 The electronic structure of conjugate polymers	10
1.3 Band theory in conjugate polymers	12
1.4 Peierls Distortion	13
1.5 Doping	14
Chapter2	19

2	Electrical property and conduction mechanism in conjugate polymers	19
2.1	Introduction	19
2.2	Elementary excitations	22
2.2.1	Solitons	22
2.2.2	Polarons and Bipolarons	23
2.3	Conduction Mechanism in polymers	26
2.3.1	Doping of conjugated polymers	26
2.3.2	Charge Transport	30
2.4	Action of external force on charge in polymers	31
	Chapter 3	33
3	Electrical property of Metal/Semiconductor (MS) and (MSM) Contact	33
3.1	Introduction	33
3.2	Energy Band Relation at Metal-Semiconductor Contact	34
3.3	Current-Voltage Characteristics	38
3.4	Impedance spectroscopy and circuit models	40
	Chapter 4	46
4	Sample Preparation and Procedures Used	46
4.1	Forming ITO/Polymer/Al sandwich	46
4.2	Measurement Techniques	48
	Chapter 5	50
5	Results and Discussion	50
5.1	Absorption Measurement	50
5.2	Current-Voltage Characteristics	52
5.3	Impedance Characteristics	58
	Conclusions	63

Appendix	64
A Thermionic Emission Theory	64
Bibliography	66

List of Tables

5.1	Electrical character of MDMO-PPV blended with fullerene	57
5.2	Electrical character of pure MDMO-PPV	58
5.3	Electrical characteristics collected form cole-cole plot of MDMO-PPV blended with fullerene	60
5.4	Electrical characteristics collected from cole-cole plot for pure MDMO-PPV	61

List of Figures

1	Conductivity of polymers compared with other materials at room temperature[4]	3
1.1	Energy schematics showing the overlap of the 1s atomic orbitals of two hydrogen atoms to form "bonding" and "anti-bonding" molecular orbitals.	6
1.2	Cylindrically symmetrical σ - bonding of a hydrogen molecule.	6
1.3	Overlap of two atomic orbitals to give a bonding of π -MO.	7
1.4	(a) Atomic ground state configuration of carbon atom, (b) its promoted configuration	8
1.5	(a) The promoted configuration of the carbon atom , (b) sp^3 hybridization and (c) the resulting tetrahedral shaped combined hybrid orbital	8
1.6	(a) The promoted electronic configuration of the carbon atom, (b) sp^2 hybridization and (c) the resulting trigonal shaped combined hybrid orbital	10
1.7	Alternating single and double bonds in conjugate polymers. PA = Polyacetylene, PT = Polythiophene, PPY = Polypyrrole	11
1.8	Possible structure for Polyacetylene chains. Two degenerate trans-structure(a)and (b), the two non-degenerate cis-structure, (c) cis-transoid and (d)trans-cisoid.	11
1.9	Two degenerate ground state configuration of trans-polyacetylene	12

1.10	Formation of the valance band and the conduction band as a result of overcrowded orbital energy levels	13
1.11	The creation of an energy gap in the dispersion relation of dimerized Polyacetylene. (a) Dispersion relation and density of state for undimerization Polyacetylene , and (b) for dimerized polyacetylene	14
1.12	Semiconductor Doped with Donor Atoms.	15
1.13	Semiconductor Doped with Acceptor Atoms	15
1.14	Equilibrating p-n Junction and direction of Photogenerated Electron and Hole	16
1.15	Substituted Polythiophene; R_1 and R_2 stands for side chain.	17
1.16	Chemical structure of some substituted polymers.	17
2.1	Comparison between band gap in metal, semiconductor and insulator . . .	20
2.2	A soliton defect at the phase boundary between the two degenerate trans phases of PA where the bond alternation has been reversed.	22
2.3	Energy band diagram of polyacetylene with solitons	23
2.4	Non-degenerate state of polythiophene. The energy of the aromatic configuration(ground state) is less than the quinoidal state energy. Hence, solitons are driven by the lattice force in the direction of arrow.	24
2.5	Formation of polaron in polythiophene	24
2.6	Bipolarons in polythiophene	25
2.7	The bond diagram of a hole polaron (left), and a hole bipolaron (right). . .	25
2.8	Formation of polaron energy band	28
2.9	Interaction of solitons to form soliton band	29
3.1	Energy band diagram of Metal- Semiconductor contact	34

3.2	Band diagram for n-type semiconductor-metal contact with $\phi_m < \phi_s$	37
3.3	Band diagram for p-type semiconductor-metal contact for (a) $\phi_m > \phi_s$, which is ohmic and (b) $\phi_m < \phi_s$, which is rectifying	37
3.4	(a) Impedance Complex plane, (b) Parallel,(c) series connection of R, X	41
3.5	Representation of (a) Z of the RC circuit in complex plane and (b) RC connected in a parallel arrangement	44
3.6	(a) Combination of resistance R_c , R and capacitance C, (b) Cole-Cole draw- ing of the impedance Z of the circuit.	45
4.1	(a) Three-dimensional view with the way charge transfer across the sample, (b) Side view showing effective area.	47
4.2	Chemical structure of MDMO-PPV and C_{60}	48
5.1	Absorption spectrum of Pure MDMO-PPV	50
5.2	Absorption spectrum of MDMO-PPV blended with C_{60}	51
5.3	Absorption spectrum of pure MDMO-PPV and blended with C_{60}	52
5.4	Current density Vs applied voltage for MDMO-PPV blended with C_{60}	53
5.5	The logarithm of current density Vs applied voltage MDMO-PPV blended with C_{60}	53
5.6	Current density Vs applied voltage for pure MDMO-PPV	54
5.7	Logarithm of Current density Vs applied voltage for pure MDMO-PPV	55
5.8	Linear part of lnJ vs V curve for Al/MDMO-PPV/ C_{60} ITO	56
5.9	Linear part of lnJ vs V curve for Al/MDMO-PPV/ITO	57
5.10	Cole-cole plot of Al/MDMO-PPV/ C_{60} /ITO	58
5.11	Cole-cole plot of Al/MDMO-PPV/ITO	59

5.12 Model of Al/MDMO-PPV/ C_{60} /ITO	60
5.13 Extrapolate for Cole-cole plot of Al/MDMO-PPV/ C_{60} /ITO	61
5.14 Extrapolate for Cole-cole plot of Al/MDMO-PPV/ITO	62

Abstract

This thesis is based on the experimental investigation of the junction between reactive low work function metal, Aluminum and Conjugated polymer, MDMO-PPV. The polymer is blended with C_{60} and the composition were also made with pure polymer. The techniques employed are absorption spectroscopy, current-voltage characteristics measurement and complex impedance spectroscopy.

The absorption measurement shows that MDMO-PPV is a semiconductor with energy band gap of about 2.0032eV. The current density-voltage curve is found to be asymmetric and non-ohmic and shows Schottky barrier type rectification. The rectification ratio of fullerene blended MDMO-PPV is found to be 100 whereas that of pure MDMO-PPV is between 10 and 20, and more diode characteristics are observed in the case of fullerene blended polymer. The complex impedance spectra are single semi-circle displaced from the origin that show the existence of mobile charge depleted regions with some contact resistance. The radius of the semi-circle is found to depend on the bias of the junction.

General Introduction

Semiconductor technology is the basis of modern electronics. It often utilizes inorganic semiconductors such as silicon. However, the use of inorganic materials for electric and optoelectronic devices require high manufacturing costs. For this and many other reasons, researchers have started to investigate alternative sources of materials. Although its birth was by chance, in recent years conducting polymers have become a new source. Historically, interest in conducting polymers grew in the past few decades because of their potential for commercial uses through the application of their novel properties such as light weight, processability, good electrical conductivity and low costs. Moreover, the prospect of applications of organic semiconductors in the areas of sensors, batteries, bio applications such as micro-muscles, large screen display, electronic and optoelectronic device, etc., have triggered considerable research activities [1]. Polymers are long chain macromolecules, made of repeating monomeric units, with a large molecular weight. The name polymer means "many parts", and is derived from the Greek word: polys- (many), meros- (parts). The term macromolecule is a synonym for polymer. The smallest part of polymer is called a monomer. A monomer is a molecule, which combines with other molecules of the same or different type to form a polymer. Oligomer refers to few monomer units. Polymers are arbitrarily arranged and have molecular weights greater than about 5000 units, but there is no firm lower limit [2]. Polymer can have different chemical structure, physical property, mechanical behavior, thermal characteristics, etc., and can be classified in different ways such as:

- Natural and Synthetic polymer
- Organic and Inorganic polymer
- Thermoplastic and Thermosetting polymer
- Plastic, Elastomers, Fibers, and Liquid resins.

Cotton, starch protein, wool etc. are examples of natural polymers, whereas nylon, rubber, fibers etc. are synthetic polymers. Most polymeric materials have been used for decades for the purpose of insulation, especially in the electronic industry. In addition, they are widely applied in application automotive, building construction and packaging.

Conjugate polymers, i.e., polymers with alternating single and double bonds, are a class of organic molecules with special properties. The basic element of an organic molecule is carbon, and a polymer contains a long sequence of consecutive carbon atoms. The carbon atoms are in turn linked together by covalent bonds (σ -bonds). The alternation of single and double bonds between consecutive carbons is called conjugation and results in a unique property, π -conjugation that is inherent in conjugate polymers. This implies that an electron can move quite freely a for certain distance (the conjugate length) along the chain. Such electrons are said to be delocalized. The conjugation arises due to the polymers ability to swap position of the single and double bonds and to result in structure that continues to satisfies the chemical bonding requirements for carbon. The delocalized electrons are called π - electrons, and they are electrons that one left behind by the formation of the repeating single and double σ - bonding. As a consequence, conjugate polymers have a unique one-dimensional character in both optical and electrical properties. The electronic conductivity of these materials depend strictly on their bond structure.

The science of solid-state physics will be the bases of the current discuss on conducting polymers. A periodic array of atoms in a lattice is essential for a high electrical conductivity. According to the band theory materials are characterized by partially filled valance band, whereas for insulators and semiconductors the valance band is filled and the conduction band is empty respectively. Electrical conductivity can also be described in terms of the density of electrons and their freedom to move. Electrical conduction of materials in any states of aggregation (solid, liquid, or gas) can be probed by applying a voltage across the material which sets up an electric field[1]. According to the response to electric field, materials can be classified as: insulators, semiconductors, conductors, or superconductors. see Fig 1. This method of classification is also valid for organic materials. Until the late 1970s, organic polymers were classified as insulators. However, the discovery that the conductivity of the conjugate polymer, polyacetylene, can be varied from insulating through semiconducting to metallic regimes by doping changes the view[3]. In the normal state, chemically pure polymers are insulators or at best semiconductors. Their conduc-

tivity is enhanced when they are oxidized or reduced, in a process known as "doping". (see Fig. 1)

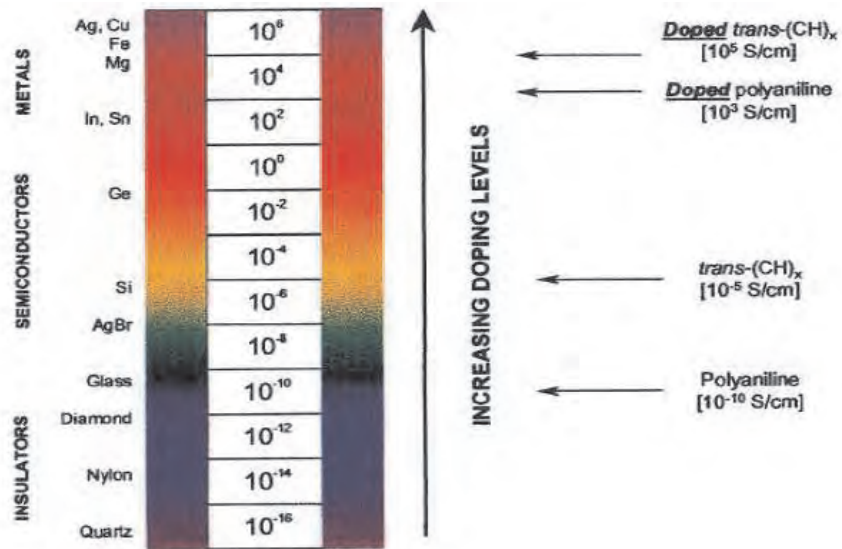


Figure 1: Conductivity of polymers compared with other materials at room temperature[4]

Undoped polymers are insulators, and have filled valance band and empty conduction band separated by a forbidden energy gap. Doping of polymers creates allowed states in the forbidden energy gap enabling the charge carriers to transit to the conduction band [5].

In this research work we studied the electrical properties of the junction between aluminium and polymers, POLY[2-METHOXY-5-(3',7'-DIMETHYLOCTYLOXY)-1, 4-PHENYLENE VINYLENE], MDMO-PPV and MDMO-PPV blended with fullerene (C_{60}). The sample was in the form of the polymers sandwiched between an Aluminum thin film and an Indium Ten oxide film electrodes. The sandwich structure device produced locally with which the investigation carried out is, of the form **Al/MDMO-PPV/ITO** and **Al/MDMO-PPV/ C_{60} /ITO**. During the research project current-voltage characteristics, the complex impedance and the absorption spectrum of both blended and pure polymers were measured in order to characterise the samples.

The thesis is organized as follows: In chapter one, the theoretical bases for the under-

standing of polymers such as how bonds are formed are presented. Chapter two, presents a brief history about conduction of conjugate polymers followed showing how conduction is possible in conjugate polymers. In the third chapter the Metal/Semiconductor(MS) and the Metal/Semiconductor/ Metal (MSM) interfaces is discussed.

Finally the forth chapter presents experimental set-up with the procedures, and the fifth chapters presents the result followed by discussion and conclusion.

Chapter 1

Chemical bonding and physics of conjugated polymers

Although organic materials play an important role as an active component in electronic devices, a number of technological factors such as long term environmental stability, processability, design, and synthesis has hindered their use. As a result, considerable research efforts have been directed to the development of new well-defined conjugate polymers and oligomers with improved processability and stability. In light of this understanding of the correlation of the physical properties with the molecular structure is of prime importance.

1.1 Molecular structure

In order to understand the molecular structure it is necessary to give a brief description of σ and π -bonds.

1.1.1 σ and π -bonds

A combination of two axioms of quantum mechanics, namely, the Heisenberg uncertainty principle and the Pauli exclusion principle, forms the basis for understanding the formation of atomic orbitals. The atomic orbitals, for example, the 1s orbital of two hydrogen

atoms, form a molecular orbital (MO) if they are brought close enough so that they overlap. The molecular orbitals that are formed encompass both of the nuclei and the electrons can move about both nuclei. There are two possible ways in which the wave functions of the electrons in both hydrogen atoms superpose to form the MOs. One of these MOs is of significantly lower energies than the sum of the energy of the original atomic orbitals. This one is known as bonding MO and it gives a stable hydrogen molecule. The other orbital, called anti-bonding, is of higher energy than the original atomic orbitals and it requires an expenditure of external energy. (See Fig 1.1).

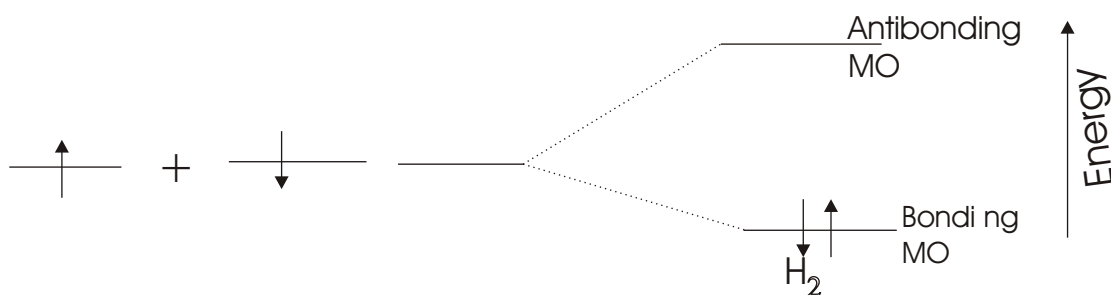


Figure 1.1: Energy schematics showing the overlap of the $1s$ atomic orbitals of two hydrogen atoms to form "bonding" and "anti-bonding" molecular orbitals.

Like an atomic orbital, a molecular orbital can be occupied by no more than two electrons. This is because of Pauli exclusion principle. When a covalent bond is formed, the two electrons originally in the atomic orbitals of the separate atoms go into the much lower energy bonding MO. The formation of the covalent bond involves the sharing of only two electrons, i.e., the pair that can be accommodated in the bonding molecular orbitals. Two different geometries are possible. The MO bonding that result in cylindrically symmetrical geometry about the line joining the two nuclei involved are called Sigma (σ) orbitals (see Fig 1.2), and the bond formed is called σ -bonds. Another type of MO bonding that can



Figure 1.2: Cylindrically symmetrical σ - bonding of a hydrogen molecule.

be formed by the overlap of the 2p orbitals is illustrated in Fig 1.3. The geometry of this second type. This MO bonding is not cylindrically symmetrical about the line joining the

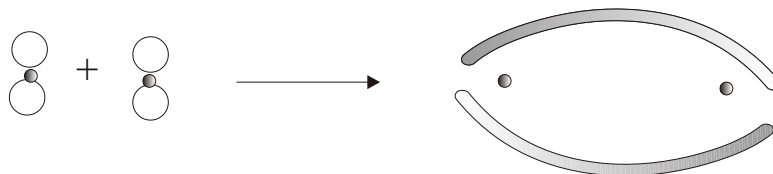


Figure 1.3: *Overlap of two atomic orbitals to give a bonding of π -MO.*

two nuclei. It is called a pi (π) bonding molecular orbital. The resulting covalent bond is called a π -bond.

1.1.2 Hybridization

Polymers are macromolecules that are constructed from repeating units called monomers connecting by covalent bonds. For conjugate polymers, and all other organic polymers, the repeating units includes carbon atoms, which have the ability to bond with other carbon atoms to form linear chains or chains of rings. The ground state configuration of carbon is $1s^2 2s^2 2p_x^1 2p_y^1 2p_z^0$, where $2s^2 2p_x^1 2p_y^1 2p_z^0$ represents the four valance electrons, see Fig 1.4a. When bonds are formed, it is more favorable for the carbon atom to promote one of the 2s electrons to the empty $2p_z$ orbitals, thus enhancing the number of bonds that can be formed, see Fig 1.4b. Electron promotion is a characteristic feature of carbon as its promotion energy is small, i.e. the energy required to increase the numbers of bonds that can be formed. The valence configuration is then changed to $1s^2 2s^1 2p_x^1 2p_y^1 2p_z^1$, having four unpaired electrons that can form single, double or triple bonds to four, three or two neighboring atoms respectively depending on the type(s) of bonding involved. Each of these three cases corresponds to a specific type of Hybridization, sp^3 , sp^2 and sp Hybridization. Orbital hybridization, in the simplest term, is simply a mathematical description that involves the superposition of individual wave functions for s and p orbitals wave function to new orbitals. The new orbitals are called "hybrid orbitals".

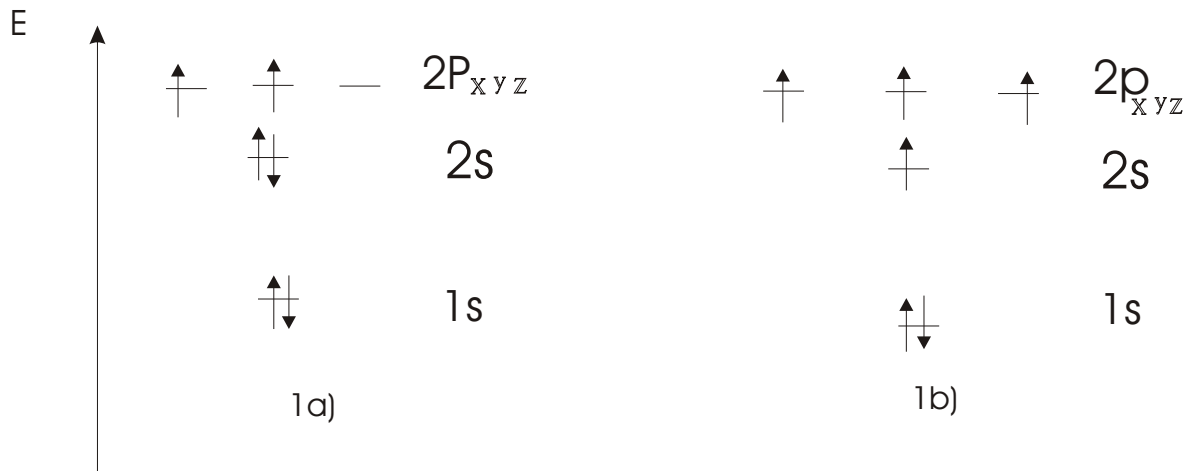


Figure 1.4: (a) Atomic ground state configuration of carbon atom, (b) its promoted configuration

1.1.2.1 sp^3 Hybridization

The carbon atoms in conventional polymers hybridize in the form of sp^3 , see Fig 1.5b. When bonding occurs, all four single occupied valance orbitals of the excited carbon atom combine into four new symmetric and equal energy sp^3 hybrid orbitals. The four hybrid orbitals form a tetrahedral shaped combination of hybrid orbitals, See fig 1.5c. Capable

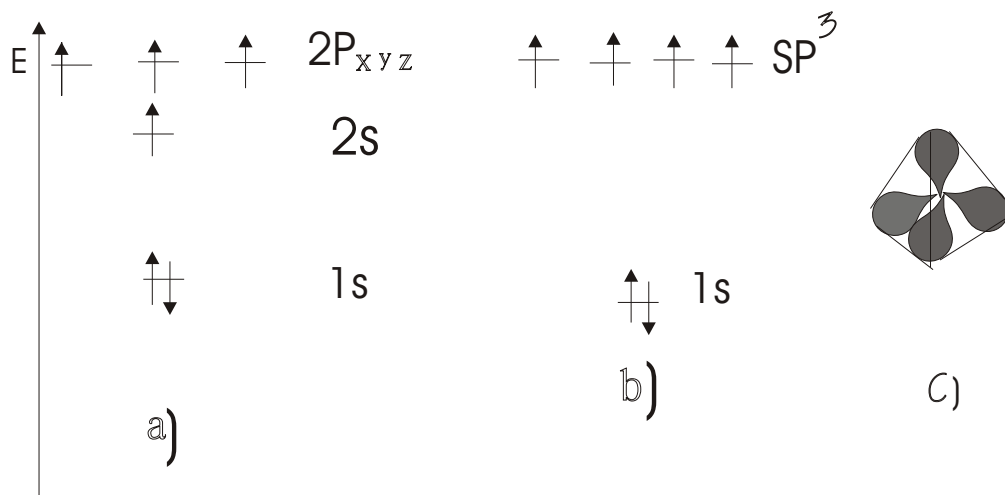


Figure 1.5: (a) The promoted configuration of the carbon atom , (b) sp^3 hybridization and (c) the resulting tetrahedral shaped combined hybrid orbital

of forming single bond to four neighboring atoms through σ bonding.

Two of these four σ bonds are formed to adjacent carbon atoms, while the remaining two σ bonds are formed to the other elements, such as hydrogen in the case of polyethylene. The electrons involved in the σ -bond along the carbon are strongly localized between the carbon atoms that they hold together. To contribute to the conduction process the electrons involved in the bonds must be free to move, the electrons involved in the σ -bonds cannot contribute to the conduction process but are bound to the atoms. This leads to the energy difference between the highest occupied molecular orbital (HOMO) and the lowest unoccupied molecular orbitals (LUMO), i.e., the energy gap E_g between them. The energy gap produced by this type of strong bonding is large, causing the materials become electrically insulating.

1.1.2.2 sp^2 Hybridization

In contrast to conventional non-conducting polymers, conducting polymers have each carbon atom sp^2 hybridized. See Fig 1.6b. When bonding occurs, the single occupied 2s orbital and two of the three single occupied 2p orbitals ($2p_x$ and $2p_y$) of the excited carbon atom combine and form three new symmetric and equal energy sp^2 hybrid orbitals. All together these three hybrid orbitals form a trigonal shaped planar combined hybrid orbital, see Fig 1.6c, capable of forming σ bonds to three neighboring atoms. As is the case for conventional polymers, the electrons involved in these σ -bond are strongly localized between the carbon atoms that hold them together, leading to the large gap between the filled σ band and the empty σ^* band. The remaining $2p_z$ orbital, which does not participate in the sp^2 hybridization, is located perpendicular to the planar combined hybrid orbitals that forms the σ -bonds and is not localized. When the $2p_z$ orbital of two adjacent carbon atoms overlap sideways they combine into two molecular orbitals. These forms the bases for the study of electronic structure of conjugated polymers.

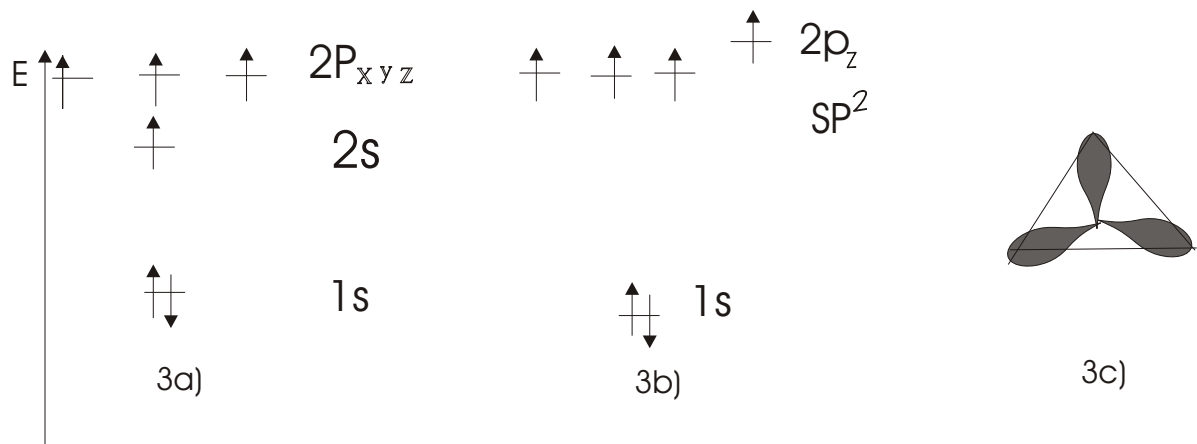


Figure 1.6: (a) The promoted electronic configuration of the carbon atom, (b) sp^2 hybridization and (c) the resulting trigonal shaped combined hybrid orbital

1.2 The electronic structure of conjugate polymers

The chain like structure of conjugate polymers has a regular sequence of strictly alternating single and double bonds (see Fig 1.7). Polyacetylene, $(CH)_n$ or PA, has the simplest, most regular, and most symmetric structure of all conjugate polymers. Its conductivity is the highest of all so far observed [1]. Hence, $(CH)_n$ is the focal point for theoretical modelling and explanation of the properties of conducting polymers. The ground state chemical structures of some conducting polymers are as shown below (Fig1.7).

Consequently, $(CH)_n$ is frequently employed to better understand the underlying physical property of conjugated polymers. The alternating bonds in polymers affect their physical and chemical properties. This can be explained as follows. As a result of electrostatic interaction between the electrons and the nuclei, the double bonds are shorter than the single bonds. Hence, double bonds are strong and localized, and therefore high conductivity is not expected along chains of alternating bonds. As a matter of fact, pure conjugated polymers are insulators or semiconductors. They need to be doped with either oxidizing or reducing agents in order to become good conductors. Thus, the alternation of bond length is responsible for the possible structure of the Polyacetylene.

There are three structures of PA. These are trans-transoid, cis-teratoid, and trans-cisoid

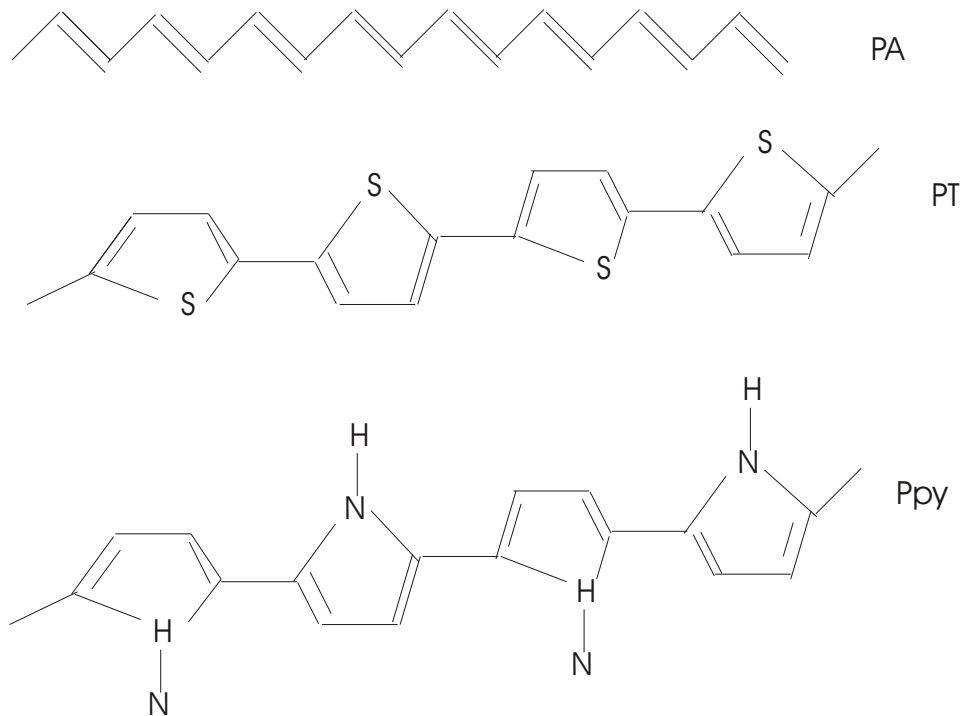


Figure 1.7: Alternating single and double bonds in conjugate polymers. PA = Polyacetylene, PT = Polythiophene, PPY = Polypyrrole

(Fig 1.8)

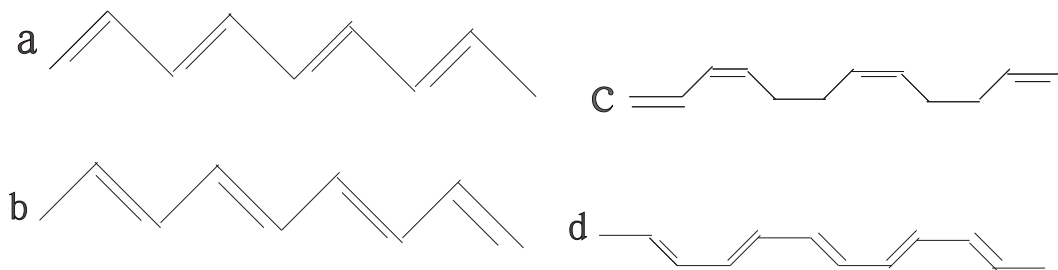


Figure 1.8: Possible structure for Polyacetylene chains. Two degenerate trans-structure (a) and (b), the two non-degenerate cis-structure, (c) cis-transoid and (d) trans-cisoid.

The cis-transoid and trans-cisoid isomers are both of high energy in contrast to the trans-transoid form and the latter is thermodynamically more stable than the other two. The trans-transoid isomer is usually called trans-Polyacetylene and it has the property that the single and double bonds can be interchanged without any loss of energy, to maintain

an equivalent chemical structure. As a result, two energetically degenerate ground state configuration of trans-PA can be formed (Fig 1.9). Cis-transoid is also simply denoted as a cis-polyacetylene. Cis-polyacetylene has a non-degenerate state. Once the bond structure

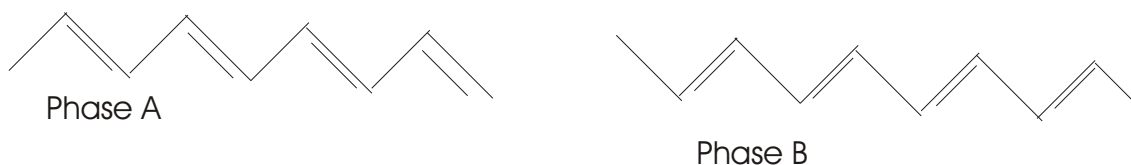


Figure 1.9: *Two degenerate ground state configuration of trans-polyacetylene*

of PA, as an example is known the electronic structure of other complex polymers can be shown. This is illustrated in the next section.

1.3 Band theory in conjugate polymers

The electronic structure of polymers depends on the nature of their bonds. The bond formation of macromolecules follows the same principle as that of the diatomic molecules. The bond formation involves the formations of two energy levels, the bonding level and the antibonding level. The energy levels before and after the bond formation are indicated in Fig 1.10. For more complex molecules, as each bond is formed, an additional bonding and antibonding level is added to the overall electron structure[6].

In large polymer molecules, thousands or millions of atoms may be involved and the number of molecular orbital is large. Beyond a certain size of the molecule the bonding orbitals bunch together on the energy scale to form a set of closely spaced energy levels. This set is known as an energy band. A similar bond formations also occurs with the anti-bonding orbitals, which are described as the conduction band[1]. In the electronic structure of organic polymers there is a large energy difference between the highest occupied molecular orbital (HOMO) and the lowest unoccupied molecular orbital (LUMO) causing electrical insulation[7]. The band theory of polymer can be helpful in the understand of semiconductivity property of the polymers.

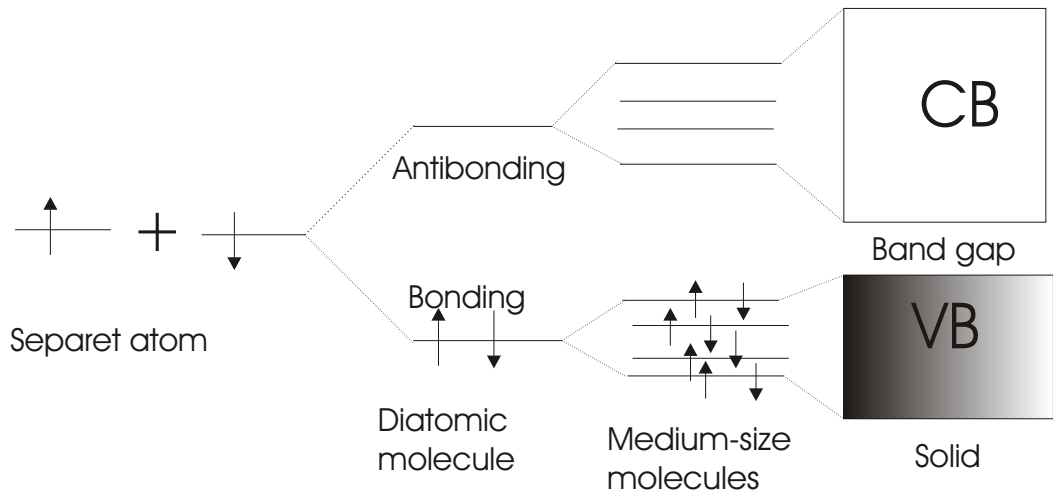


Figure 1.10: *Formation of the valance band and the conduction band as a result of overcrowded orbital energy levels*

1.4 Peierls Distortion

Normally carbon atoms form the backbone of conjugated polymers in sp^2 hybridization, because it possess one free electron from the $2p_z$ which is not bonded with other nearest atoms. This p_z orbital interacts with its neighbor, forming a π - bond between the atoms. Since the inter-chain coupling in these system is weak, one can assume that PA has an extended chain with bond angle of 180° [1], then the main chain can be considered as a one dimensional lattice. But according to solid state physics, the electronic-state of a one-dimensional system with one free electron per unit cell (i.e., first Brillouin zone) has half-filled energy bands and the material can be considered as metals. However, these materials are not stable as a metal; a one-dimensional system with a half-filled energy band is unstable and will undergo a transition to a dimerized state[25], and so that the carbon-carbon bond will be distorted by alternating double and single bonds of the linear chain. This distortion is called Peierls distortion, and it changes the unit cell of the polymer to contain two CH groups, and allows a transition in the total energy of the system by creating a band gap (see Fig.2.6 a), with the π -conjugated system and the material exhibits semiconducting properties instead of metallic[13].

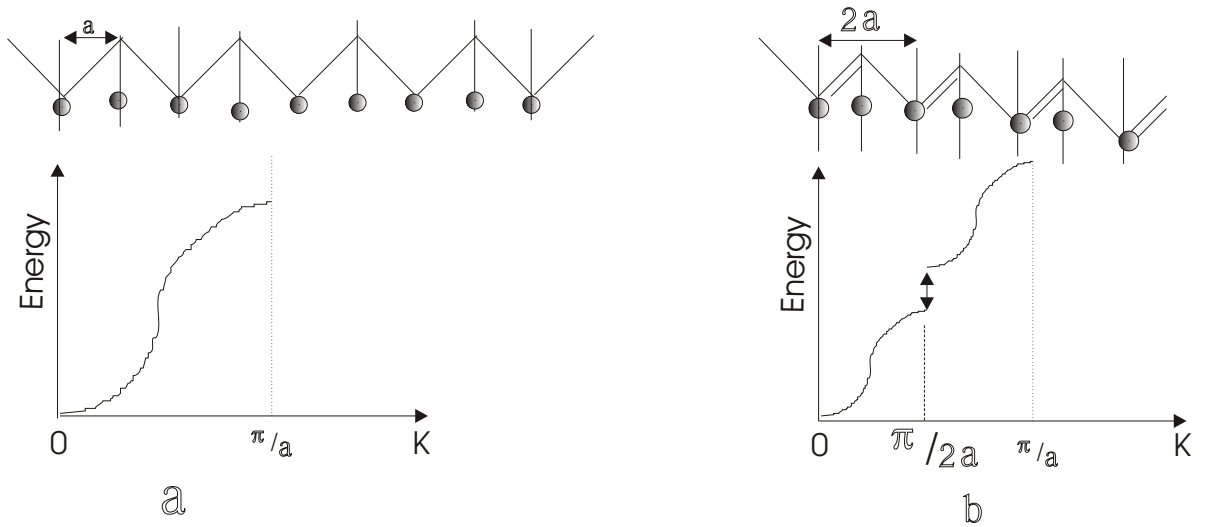


Figure 1.11: *The creation of an energy gap in the dispersion relation of dimerized Polyacetylene. (a) Dispersion relation and density of state for undimerization Polyacetylene, and (b) for dimerized polyacetylene.*

A Peierl's distortion is a disorder-to-order phase transition in the electronic system, and it leads to the energy gap in the dispersion relation (see Fig.1.11b) [11]. Several conjugate polymers have E_g varying from 0.7eV to 3eV. For example, from optical measurement, the energy band gap of polyacetylene is 1.7eV [15]. But most other conjugate polymers have values higher than 1.7eV. Due to this their intrinsic conductivity is very low. To obtain high conductivity they need be doped.

1.5 Doping

Doping is a process of deliberately incorporating of impurity atoms into a materials. For example, conventional photovoltaic are fabricated from silicon or gallium arsenide based materials which consists of n-type and p-type semiconductor. The former consists of an intrinsic semiconductor doped with a donor element (i.e, atom with negative valance), while the latter is doped with an acceptor element (atom with positive valance). Let us first discuss doping in silicon since it has a simple lattice structure. In silicon crystal each atom makes covalent bonds with the surrounding four nearest host atoms. If one

of the silicon atom is replaced by phosphorous for example, an electron will be free after forming covalent bonds with the remaining four nearest silicon atoms. This free electron contributes to the conduction and hence the material is known as n-type. On the other

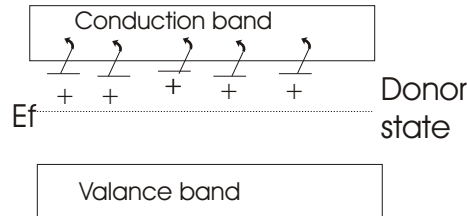


Figure 1.12: *Semiconductor Doped with Donor Atoms.*

hand, if the silicon atom is replaced by an acceptor atom like boron, there will be a deficiency of an electron when boron makes bond with three nearest silicon atoms. Such incomplete bonding leave behind a hole in the valance band causing the material to be p-type. Electrical conduction in p-type materials is carried out by the movement of holes in the valance band. Holes are charge carriers left behind as a result of electron removal from a system.

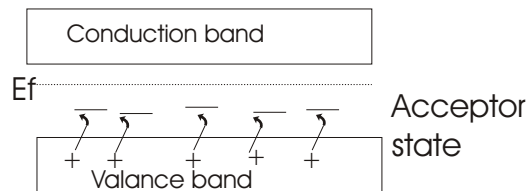


Figure 1.13: *Semiconductor Doped with Acceptor Atoms .*

Electrons in n-type materials and holes in p-type materials are known as majority carriers since they are the mechanisms of conduction. The majority carrier concentration is determined solely by the doping concentration. On the other hand, minority carrier concentration is determined by external excitation such as photon absorption or thermal excitation. If a pn junction is formed by placing a n-type semiconductor next to a p-type semiconductor, excess majority carriers will diffuse across the junction. Diffusing electrons leave behind positively charged donor atoms and diffusing holes leave behind

negatively charged acceptor atoms. The separation of charges create an electric field across the junction which opposes the force created by the concentration gradient. In equilibrium, the diffusion force matches the force due to the induced electric field and a depletion region is formed at the pn junction. The n-type semiconductor already has an

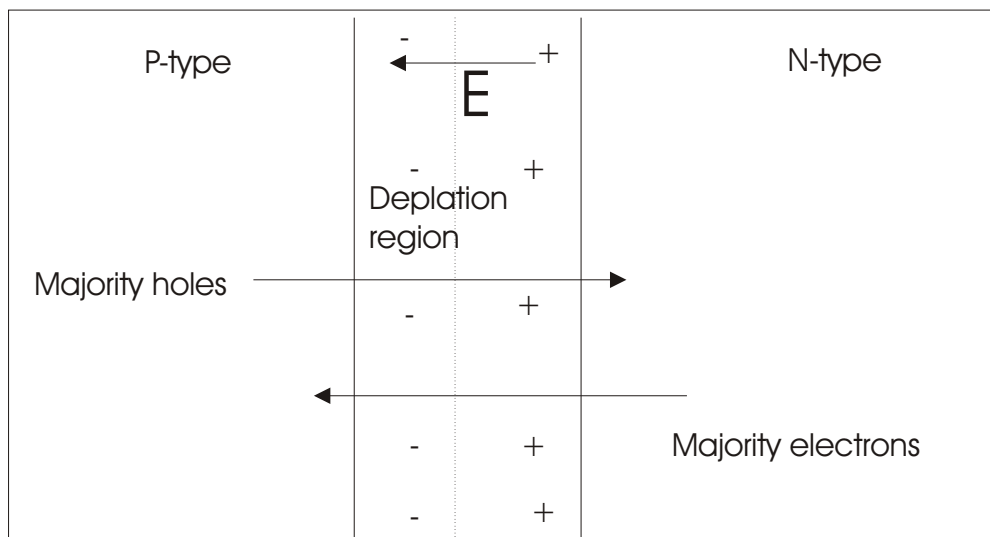


Figure 1.14: *Equilibrating p-n Junction and direction of Photogenerated Electron and Hole*

excess of electrons and the p-type semiconductor has an excess of holes. If an alternating current path is provided, connecting the n-type and p-type semiconductors together, the exciton electrons will flow back to the p-type semiconductor and exciton holes will flow back to the n-type semiconductor. This provides a current. The electric field across the depletion region provides a driving voltage. Together current and voltage provide power.

In inorganic semiconductors doping involves replacing some of the atoms with different species of atoms, while in conducting polymers there is no replacement of any atoms of the polymer (briefly discussed in 2.3.1), rather the dopant simply act as associates that accept or donate electrons[8]. Doping of polymers may be carried out chemically or electrochemically to reach desired levels of conductivity. An important class of polyconjugated materials consists of the heterocyclic polymers such as Polythiophene, PT, (and its derivative), and Polypyrrole, PPY, PPV, and other polymers with heteroatoms in the main chain, for example polyaniline, PANI. Some polymers, such as PPY and PANI, can

be directly synthesized in their doped states. Different heterocyclic structures have been

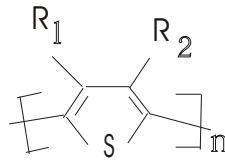


Figure 1.15: *Substituted Polythiophene; R_1 and R_2 stands for side chain.*

introduced to decrease the band gap of the conjugate polymers[1]. In polythiophene, for example, a variety of side chain substituents attached to the 3- and 4-positions (see Fig. 1.15) gives rise to modified electronic properties. Some substituted polythiophenes are

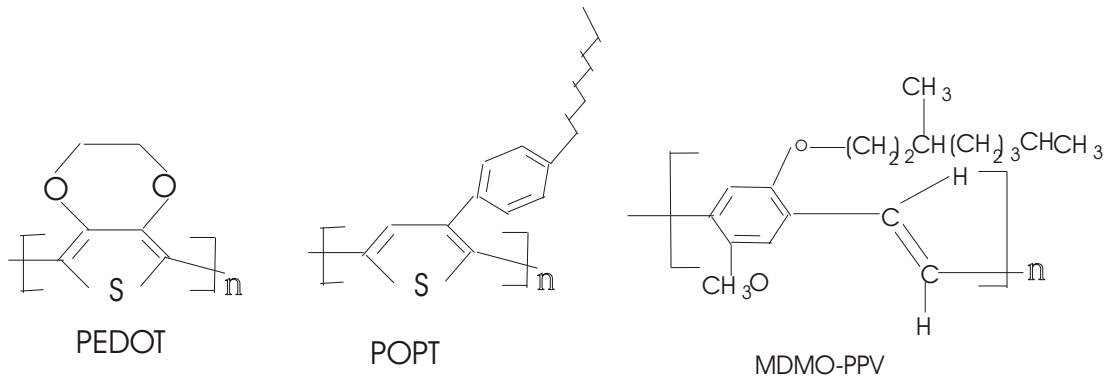


Figure 1.16: *Chemical structure of some substituted polymers.*

depicted in Fig. 1.16.

Some applications of conductive polymers[4]

Doped polyaniline is used as a conductor and for electromagnetic shielding of electronic circuits. Polyaniline is also manufactured as a corrosion inhibitor.

Poly(ethylenedioxythiophene) (PEDOT) doped with polystyrenesulfonic acid is manufactured as an antistatic coating material to prevent electrical discharge exposure on photographic emulsions and also serves as a hole injecting electrode material in polymer light-emitting devices.

Poly(phenylene vinylidene) derivatives have been major candidates for the active layer in pilot production of electroluminescent displays (mobile telephone displays).

Poly(dialkylfluorene) derivatives are used as the emissive layer in full-colour video matrix displays.

Poly(thiophene) derivatives are promising for field-effect transistors: They have potential for use in supermarket checkouts.

Poly(pyrrole) has been tested as microwave-absorbing stealth (radar-invisible) screen coatings and also as the active thin layer of various sensing devices.

Chapter 2

Electrical property and conduction mechanism in conjugate polymers

2.1 Introduction

About 45 years ago all carbon based polymers were mainly regarded as an insulators. Their low electrical conductivity is the unique property that distinguish as them from metals and inorganic semiconductors. In fact, the insulating properties of the polymer is traditionally utilized to insulate electrical wires. It is a general view that plastics and electrical conductivity are mutually exclusive. Since the past 15 years, however, a new class of organic polymers have been discovered with the remarkable ability to conduct electric current[4]. Part of a larger class of materials called "synthetic metals," some of these conducting plastics are already under development for practical applications, such as rechargeable batteries, electrolytic capacitors, and "smart windows" that absorb sunlight in summer. The synthetic materials have tremendous potential for future scientific and technological development. Excitement about these relatively new materials is high because a plethora of new, often exotic, applications may become reality. The novel property of the conducting polymers that can be used for different applications has brought together Scientists from traditionally different areas such as chemistry, physics, electrical engineering, and material science, to work toward a common goal in designing

and controlling the electrical and mechanical properties of these materials. As a result, research in the field of conductive polymers is highly interdisciplinary. A major obstacle, however, to the rapid development of conductive polymers is the lack of understanding of how electrical transport in them. All conductive polymers have one feather in common: they contain extended π -conjugated systems with single and double bonds alternating along the polymers chain. The main goal in this field is to understand the relationship between the chemical structure of the repeating unit of the polymer and its electrical properties. Such understanding would enable the electronic and mechanical properties of these materials to be studied at the molecular level.

The theory that most reasonably explains the electronic properties of materials is based on the energy band concept. In the solid state, the atomic orbitals of each atom overlap with the same orbitals of their neighboring atoms in all directions to produce molecular orbitals similar to those in small molecules. The number of atomic orbitals in a solid is about 10^{22} per cc[4] , and thus similar amounts of molecular orbitals are also expected in solid polymers. When this many orbitals exist in a given range of energies, they form appear to form continuous energy bands. The energy spacing between the highest occupied and

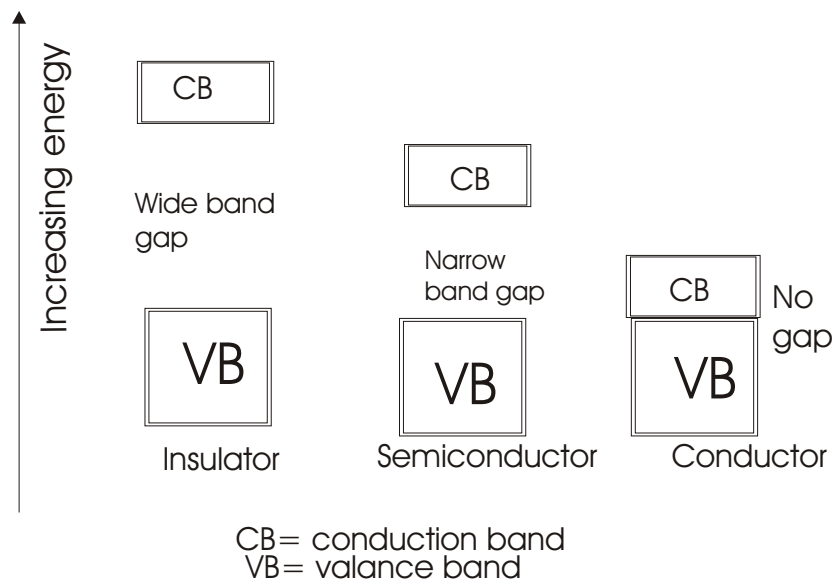


Figure 2.1: Comparison between band gap in metal, semiconductor and insulator

lowest uncoupled bands is called the band gap. This energy gap is wider for insulators and narrow for metals [4].(see Fig. 2.1).

According to energy band theory, electrical properties of materials depend on the shape of the band and distribution of charges across the band. When the energy bands overlap the conductivity is very, as in the case of metals. When the bands are filled or empty, no conduction occurs. If the band gap is small, thermal excitation of electrons from the valance band to the conduction band at room temperature gives rise to higher conductivity. When the band gap is too wide, thermal excitation at room temperature is insufficient to excite electrons across the gap and hence the material is an insulator. This is the case in inorganic semiconductors.

Conductive polymers are peculiar in that they conduct current without having a partially empty or partially filled band. Their electrical conductivity cannot be explained well by simple band theory. For example, simple band theory cannot explain why the charge carriers, usually electrons or holes, in polyacetylene and polypprol have zero spin. To explain some of the electronic phenomena in organic polymers, new particles nature such as solitions, polarons, and bipolarons (quasi-particles), have been described to explain conducting polymers. When an electron is removed from the top of the valance band of a conjugated polymer, such as polyacetylene or polypprole, a vacancy (hole or radical cation) is created that does not delocalize completely, as would be expected from classical band theory. Only partial delocalization occurs, extending over several monomeric units and causing them to deform structurally. The energy level associated with this radical cation represents a destabilized bonding orbital and thus has a higher energy than the energies in the valance band. In other words, its energy lies in the band gap. This rise in energy is similar to the rise in energy that takes place after an electron is removed from a filled bonding molecular orbital. In solid-state physics, a radical cation that is partially delocalized over some polymer segment is called a polaron. The polaron stabilises itself by polarizing the medium around it hence the name. Thus knowing the nature of an elementary excitation, one can better explains the way conduction occurs in polymers.

2.2 Elementary excitations

2.2.1 Solitons

As we saw in chapter one, PA has two degenerate ground states which are denoted by phase A and phase B (Fig 1.9). Due to degeneracy double and single bonds can be interchanged without changing the ground state energy of the system. If these two chains are put together a phase transition can occur where the two phases have a misfit as shown in the Fig 2.2.

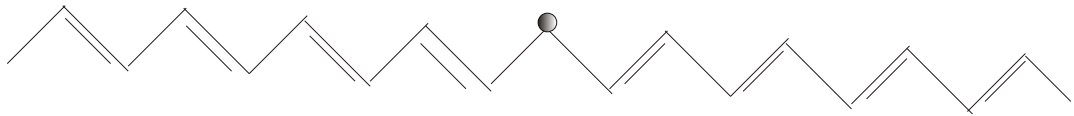


Figure 2.2: A soliton defect at the phase boundary between the two degenerate trans phases of PA where the bond alternation has been reversed.

Considering the bonding of carbon atoms on the chain where the defect occurs, the carbon atom between the segments will be sp^3 hybridized and contains one unpaired electron although the overall charge remains zero. Therefore, this defect site has zero charge, but spin $\frac{1}{2}$. Moreover, addition of an extra electron to, or removal of an electron from the defect, makes the spin of the non-bonding state zero, and hence the charge becomes $\pm e$. Consequently, a new state (energy level) is created in the energy band gap (i.e the unpaired electron resides in a non-bonding orbitals)(see Fig 2.3). This neutral defect is known as a soliton [9, 10]

A soliton separates a segment of polymer chain with two phases as shown in the Fig 2.2. Therefore, the soliton in PA is a bond alteration "domain wall", a localized region on the chain where the bond alteration reverses. The neutral soliton is single occupied has a spin $\frac{1}{2}$, and has been calculated to be delocalized over about 15 carbon atoms [9]. Charged solitons can be created by doping the polymer. chemically oxidizing or reducing the polymer adds or removes the charges from the polymer chain creates a structural defect known as charged solitons. A new energy level in the forbidden energy gap is

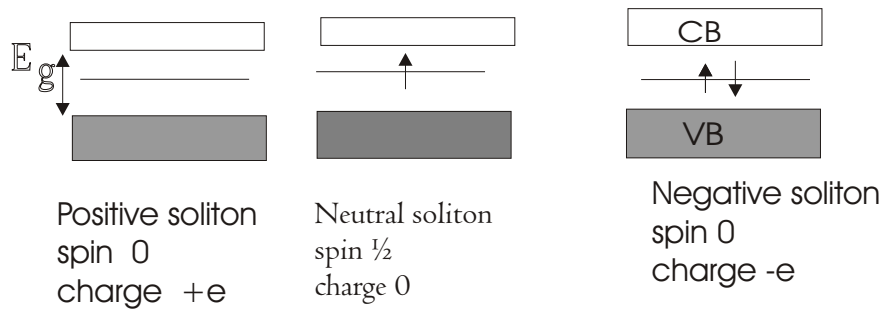


Figure 2.3: Energy band diagram of polyacetylene with solitons

also created (see Fig.2.3)[11]. The soliton energy state can contain either zero (positively charged soliton), one(neutral soliton) or two (negatively charged soliton) electrons.

2.2.2 Polarons and Bipolarons

The motion of electrons in an ionic crystals gives rise to another quasi particle. When an electron is moving in an ionic crystal, its surrounding medium will be polarized, with negative ions being repelled and positive ions being attracted toward it. The polarized field thus produced, in turn, affects the motion of the electron itself. This moving electron with its accompanying polarization field is known as a Polarons[14]. A polaron is a charge carrier[1]. Two classes of polarons are generally identified. These are the small and the large polarons. In small polarons, the size of the polarons is comparable to the lattice constant, and the electron-phonon coupling is very strong. Large polarons have relatively weak coupling and large size.

By the same analogy the term polarons in conjugated polymers is used to represent a local electron state and associated lattice distortion. It is described as a bound state of soliton and anti-soliton[1]. There are many ways that a polaron can be created in conjugate polymers. Polarons can be formed in non-degenerate organic molecules. Polyacetylene has degenerate ground state (section 1.2). However, many other conjugate polymers have non-degenerate ground state. For instance, the left and the right side of the solitons in polythiophene, as shown below (Fig. 2.4) have different energies.

In polyacetylene, it does not matter whether the double bond is on the negative or positive

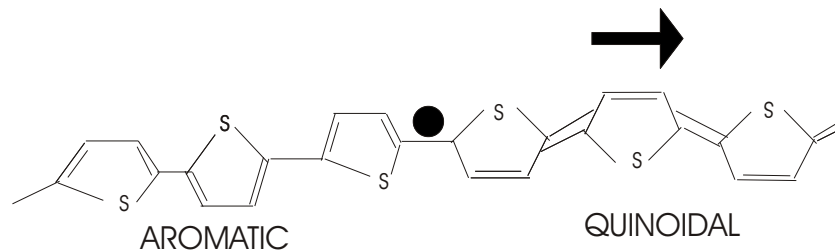


Figure 2.4: *Non-degenerate state of polythiophene. The energy of the aromatic configuration (ground state) is less than the quinoidal state energy. Hence, solitons are driven by the lattice force in the direction of arrow.*

slopes. However, in polythiophene, breaking the conjugate at the misfit leads to the transition from aromatic (two double bonds in the rings and a single bond between the rings) to a quinoidal state (with only one double bond in the rings and a double bond separating the rings). The quinoidal state has higher energy than the aromatic state. Thus, the soliton separates regions of high and low energy.

Contrary to the soliton in polyacetylene, which are more stable and can be positioned anywhere in the chain, solitons in the non-degenerate polymers are energetically unstable. Thus they move to the end of the chain, thereby changing the high energy quinoidal ring to low energy aromatic rings. If non-degenerate ground states are to be stable, bound double-defects must be created, (see Fig. 2.5). This bound double-defect is what is known as polaron.

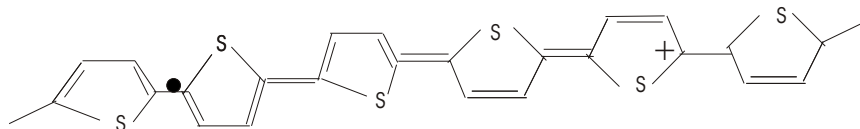


Figure 2.5: *Formation of polaron in polythiophene*

The formation of polarons is regarded as a creation of two solitons in a single chain. These two defects are pushed by the lattice force and migrate to each other, minimizing the energy. In the formation of such solitons one of them must be neutral. If the other is a positive soliton, then they form a (hole) polaron, see fig 2.5. In the event that both

solitons are positive, they form a quasi-particle known as a bipolaron. Usually bipolarons are said to be formed when two polarons meet, (see Fig 2.7). Bipolarons are more stable than two polarons: in other words the sum of two energies of two polarons is greater than the energy of bipolaron. Polarons attract each other bipolarons repel each other, but polarons and bipolarons coexist[1].

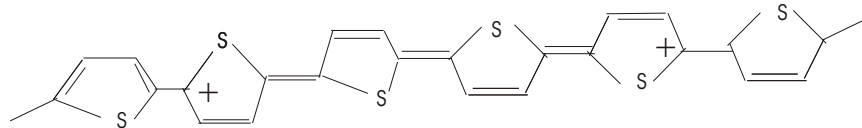


Figure 2.6: *Bipolarons in polythiophene*

Generation of polarons and bipolarons creates two interacting states which are energetically separated in the energy gap, unlike the single state of the solitons. Fig. 2.7 shows the energy band diagram of the polaron and bipolaron states. For polarons each level within the gap is singly charged, while for bipolarons all the states are empty or full which implies that bipolarons are spinless.

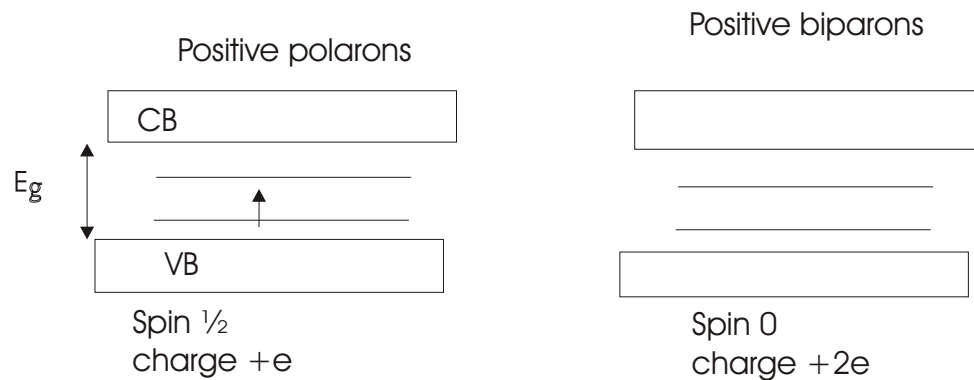


Figure 2.7: *The band diagram of a hole polaron (left), and a hole bipolaron (right).*

From figure 2.7, we observe that the positive bipolarons makes possible a new transition, namely a transition from the valence band to two different bipolaron states. From the discussion in the last subsection the conclusion can be made that the conduction mechanism in polymers is mainly due to these elementary excitations.

2.3 Conduction Mechanism in polymers

2.3.1 Doping of conjugated polymers

The properties of conjugated polymers can be changed drastically by addition or subtraction of electrons to or from the conjugated polymer chain, with simultaneous interaction of the compensating counter ions between the chains. This process is called doping[12]. The polymer may be doped with either acceptor or donor impurity atoms. This is similar to the doping of silicon based semiconductors where silicon is doped with either arsenic (donor) or boron (acceptor). However, while the doping of silicon produces a donor energy level close to the conduction band or acceptor level close to the the valance band (as discussed in section 1.4), this is not the case with conducting polymers. The evidence for this is that the resulting polymers do not have a high enough concentration of free spins, as determined by electron spin spectroscopy[12]. Initially the free spin concentration increases with the concentration of the dopant. At larger concentration, however, the concentration of the free spins levels off at maximum. To understand this it is necessary to examine how charge is stored along the polymer chain and its effects.

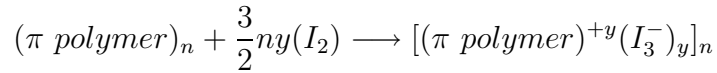
Polymers may store charge in two ways. In an oxidation process it could either lose an electron from one of the bands or it could localize the charge over a small section of the chain. Localizing the charge causes a local distortion due a change in geometry, which costs the polymer energy. However, the generation of this local geometry decreases the ionization energy of the polymer chain and increases its electron affinity making it more able to accommodate the newly formed charges. This method increases the energy of the polymer less than if the charge was delocalized, and hence takes place in preference to charge delocalization. This is consistent with an increase in disorder detected after doping as observed by Raman spectroscopy. A similar scenario occurs for a reduction process. Doping can be done in many ways such as [12]

- Chemical doping by charge transfer
- Electrochemical doping
- Doping of polymer by acid base chemistry

- Photodoping
- Charge injection at a metal semiconductor polymer interface.

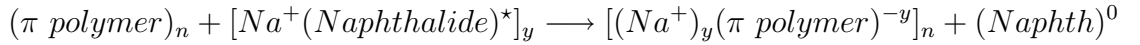
In chemical doping typically the oxidizing dopants used includes iodine, arsenic pentachloride, iron(III)chloride and $NOPF_6$. A typical reductive dopant is sodium naphthalide. The main criteria of a suitable dopant is its ability to oxidize or reduce the polymer without lowering its stability. Besides, the dopant should not initiate side reaction that hinders the polymer electrical conductivity. Chemical doping can be generalized as follows[4] .

a). P-type doping,



Here the polymer gains an extra electron that can move along the polymer chain.

b). n-type doping



Unlike the P-type doping, here the polymer loses one electron and hence hole is created that can contribute to conduction.

The oxidative doping of polypyrrole proceeds in the following way. An electron is removed from the p-system of the backbone chain producing a free radical and a positive charge. The radical and cation are coupled to each other via local resonance of the charge and the radical. In this case, a sequence of quinoid-like rings are used. The distortion produced by this is of higher energy than the remaining portion of the chain. The creation and separation of these defects cost considerable amounts of energy. This in turn limits the number of quinoid-like rings that can link these two bond species together. The combination of a charge site and a radical is called polaron. This could be either a radical cation or radical anion. A new localized electronic state is created in the gap, with the lower energy state being occupied by a single unpaired electron. (see Fig.2.8)

Upon further oxidation the free radical of the polaron is removed creating a new spinless

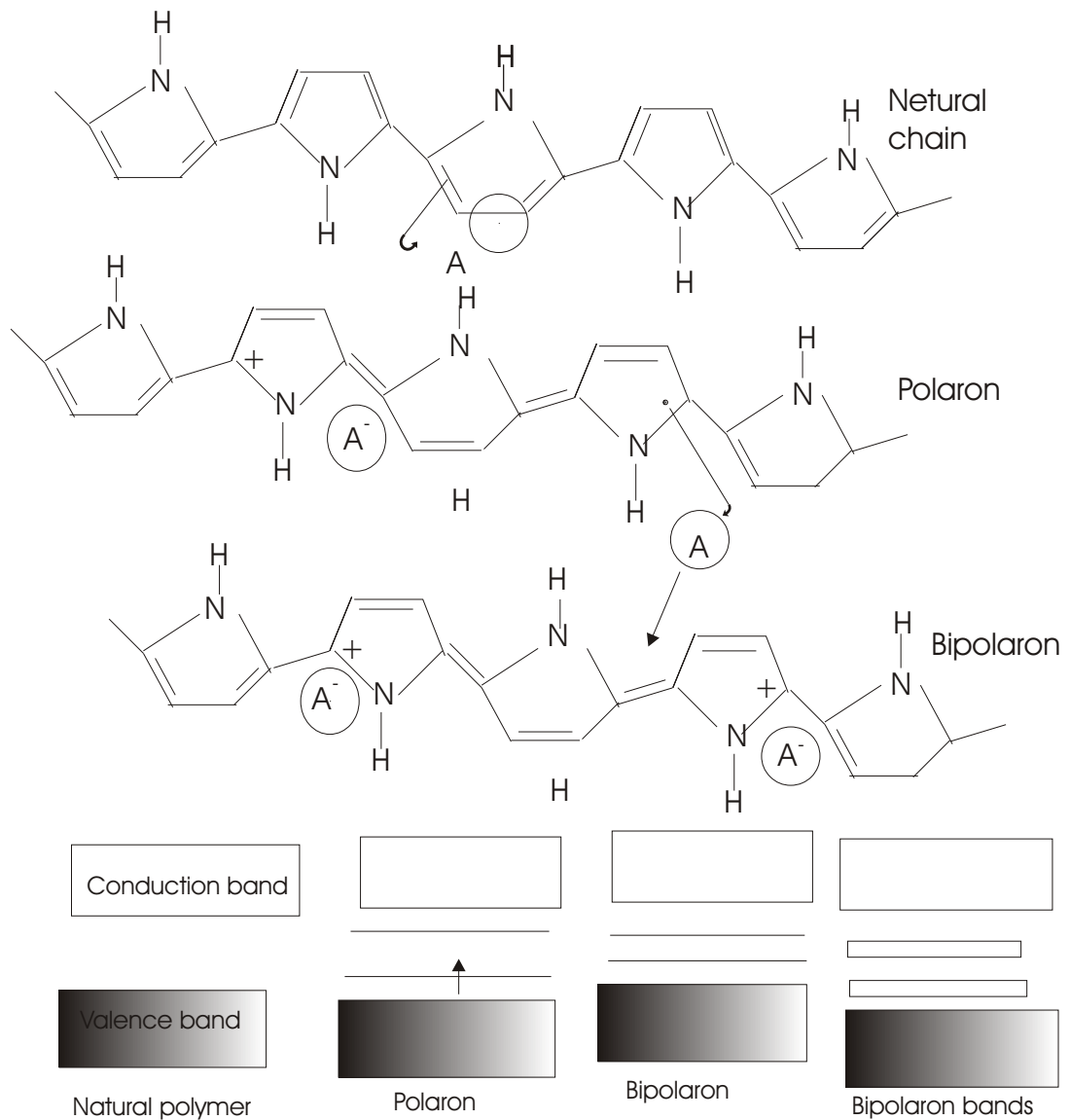


Figure 2.8: *Formation of polaron energy band*

defect called a bipolaron. Bipolaron formation requires lower energy than the creation of two distinct polarons. At higher dopant levels two polarons combine to form a bipolaron. Thus, at higher dopant level the polarons are replaced by bipolarons. Eventually, with continued doping continuous bipolaron bands are formed. Their band gap also increases as newly formed bipolarons are made at the expense of the band edges. For very heavily doped polymers it is conceivable that the upper and the lower bipolaron bands will merge with the conduction and the valence bands respectively to produce partially filled bands

and metallic like conductivity. (see Fig. 2.8)

Conjugated polymers with a degenerate ground state have a slightly different mechanism. As with polypryrole, polarons and bipolarons are produced upon oxidation. However, because the ground state structure of such polymers are twofold degenerate, the charged cations are not bound to each other by a higher energy bonding configuration and can freely separate along the chain. The effect of this is that the charged defects are independent of one another and can form domain walls that separate two phases of opposite orientation and identical energy. These are called solitons and can sometimes be neutral. Solitons produced in polyacetylene are believed to be delocalized over about 12 CH units

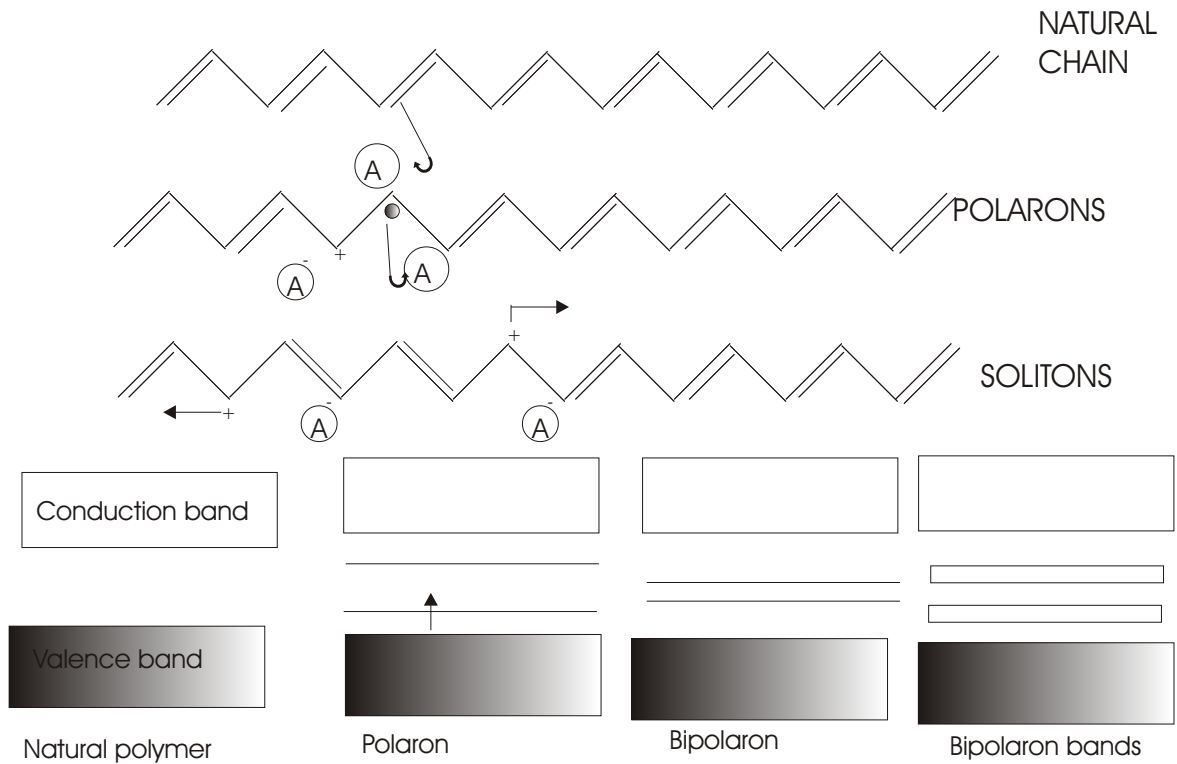


Figure 2.9: *Interaction of solitons to form soliton band*

with the maximum charge density next to the dopant counter ion. The bonds closer to the defect show less amount of bond alternation than the bonds away from the center. Soliton formation results in the creation of new localized electronic states that appear in the middle of the energy gap. At high doping levels, the charged solitons interact with

each other to form a soliton band which can eventually merge with the band edges to create true metallic conductivity. This is shown Fig 2.9.

2.3.2 Charge Transport

Although solitons and bipolarons are known to be the main source of charge carriers in polymers, the precise conduction mechanism is not yet fully understood. The problem lies in attempting to trace the path of the charge carriers through the polymer. Polymers are generally highly disordered, containing a mixture of crystalline and amorphous regions. It is necessary to consider the transport along and between the polymer chains and also the complex boundaries established by the multiple number of phases. This has been studied by examining the effect of doping, with temperature, with magnetism and the frequency of the current used. These test show that a variety of conduction mechanisms are employed. Charge transport mechanism is mainly the movement of charge carriers between localized sites or between solitons, polarons or bipolarons states. Alternatively, inhomogeneous doping could also produce metallic island dispersed in an insulating matrix, thus conduction can take place by the movement of charge carriers between highly conducting domains. Charge transfer between these conducting domains also occurs by thermally activated hopping (phonon-assisted quantum tunneling) or tunneling. This is of course consistent with the observed rise in conductivity with temperature. In fact, at high temperatures more phonons are available which can assist the hopping. On the other hand, lowering the temperature of the polymer freezes out phonons and consequently decreases the electrical conductivity. The average hopping will decrease as a temperature decrease and this phenomena is known as "variable range hopping". The tunneling probability decreases exponentially with distance, which results in an exponential decrease in the conductivity. Temperature dependant conductivity can be written as [15].

$$\sigma = \sigma_0 \exp\left[-\left(\frac{T_0}{T}\right)^\gamma\right] \quad (2.1)$$

Where γ depends on the dimensionality d of the hopping process and is given by

$$\gamma = \frac{1}{1+d}, \quad (2.2)$$

$$\sigma_0 = e^2 N(E_f) \left[\frac{8}{9} \pi \alpha N(E_f) kT \right]^{-\gamma}, \quad (2.3)$$

and

$$T_0 = \frac{(8\alpha)^3}{9\pi k N(E_f)}.$$

For three-dimensional variable hopping, $\gamma = \frac{1}{4}$ and eq.(2.1) is Mott's famous $T^{(-\frac{1}{4})}$ law at low temperature[16]. In these equations T is a temperature in degrees Kelvin. As expected for a semiconductor the conductivity decreases with decreasing temperature (to zero at T=0) as a result of the decreasing thermal excitations of electrons. By contrast, for metals the conductivity increases with decreasing temperature[4].

2.4 Action of external force on charge in polymers

In inorganic semiconductors, the photogeneration of charge involves the excitation of the charge from the valance band to the conduction band by the application of a photon source. Due to the delocalization of the electronic state and screening effects, the resulting weak coulomb interactions between electron-hole pair carriers are either negligible or form very weakly bound excitations.

In conjugate polymers, the π -conjugated system extends over the whole polymer chain, thus allowing for delocalized states in one direction. Therefore, conjugated polymers were initially regarded as one-dimensional semiconductors[12].

The primary photoexcited species in a conjugated polymers is a neutral electron hole pair called an exciton, which is the result of the electron-electron interaction in an excited state of the conjugated polymer. From the point of view of binding energy, excitons can be classified as Columbic excitons and polaronic excitons. In Columbic excitons, the electron-hole pair are bound by their coulombic interaction. In the sprit of constructing a bipolaron, one can think of constructing a polaronic exciton by coupling two opposite

charges thereby confining a segment of the energy structure. This results in a neutral excitation with spin 0 or 1.

An exciton is bound together due to a Coulombic attraction between the two oppositely charged particles. However, if an exciton is generated near enough so it can diffuse into the depletion region before recombining, the regions electric field will split the exciton and drive the electron towards the n-type material and the hole towards the p-type material, provided that the charge carriers do have enough energy to cross the band gap.

Most conjugate polymers have energy band gaps ranging from 0.7 up to 3eV, which means that they are ideal materials for optoelectronic devices that work in the visible range of electromagnetic spectrum. Photogeneration of free carrier in conjugated polymers is a two-step process involving creation of an exciton due to the incident photon, and subsequent dissociation of these excitons into free electrons and holes. These excitons migrate along the chain before dissociation into free electrons and holes. The exciton migration of the excitons varies from 5 nm to 10 nm for different conjugate polymers before dissociation[12]. The interchain migration results in the lowering of the energy of the exciton before it emits or dissociates. The exciton dissociation can be achieved by applying an external electric field or by an electric field at the interface involving the conjugate polymer/metal interface. The simplest interface is created at the junction between the electrode and the conjugated polymer[12]. Under open-circuit condition, holes are collected at the high work function electrode (for example indium tin oxide, ITO) and electrons are collected at the low work function electrode (such as aluminum).

Chapter 3

Electrical property of Metal/Semiconductor (MS) and (MSM) Contact

3.1 Introduction

The earliest systematic investigation on the metal-semiconductor rectifying system is generally attributed to Braun who in 1874 noted the dependence of the total resistance on the polarity of the applied voltage and on the detailed surface conduction[23]. The point-contact rectifier in various forms found practical applications beginning in 1904. In 1913 Wilson formulated the transport theory of semiconductors based on the theory of solids[23]. This theory was then applied to the metal-semiconductor contact. In 1938 Schottky suggested that the potential barrier could arise from the space charges in the semiconductors alone without the presence of a chemical layer. The model arising from this consideration is known as the Schottky barrier[23].

3.2 Energy Band Relation at Metal-Semiconductor Contact

When two different conducting materials are in intimate contact, the energy band edge near the interface will be discontinuous. This is due to the fact that materials generally do not have the same energy band gap. That is, the position of the Fermi-level of the two materials are different before contact is made. After contact, however, the Fermi-level in the two materials must be coincident at thermal equilibrium. To this end, assume that a metal of work function ϕ_m is to be in contact with an n-type semiconductor, as shown in Fig.3.1. The work function of a metal is the minimum energy necessary for an electron to escape in to vacuum from an initial energy at the Fermi-level, $q\phi_m$ (ϕ_m in volt).

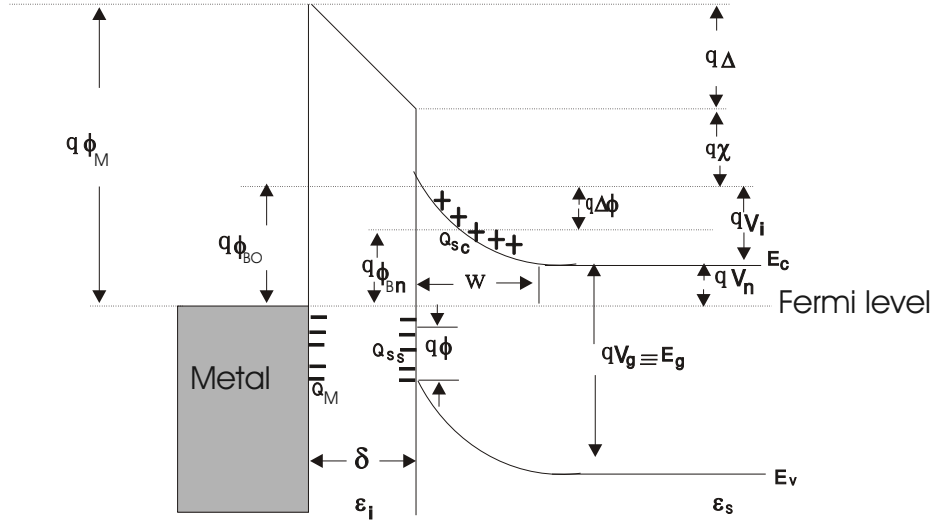


Figure 3.1: Energy band diagram of Metal- Semiconductor contact

Where

$q\phi_m$ = the work function of the metal.

$q\phi_s$ = the work function of the semiconductor.

$q\phi_{Bn}$ = the barrier height of metal- semiconductor barrier

$q\phi_{B0}$ = the asymptotic value of $q\phi_{Bn}$ at zero electric field

$q\phi_0$ = the energy level at the surface

$q\Delta\phi$ = the image force barrier lowering

Δ = the potential across the interfacial layer
 χ = the electron affinity of the semiconductor
 V_b = the built-in potential
 ϵ_s = Permittivity of semiconductor
 ϵ_i = the permittivity of interfacial layer
 δ = the thickness of the interfacial layer
 Q_{sc} = the space-charge density in the semiconductor
 Q_{ss} = the surface-state density on semiconductor
 Q_m = the surface-charge density on metal

Here, the junction built in potential V_b is the barrier height electrons needs to overcome when moving from the semiconductor to the metal, and ϕ_B is the barrier height electrons needs to overcome when moving from the metal to the semiconductor and q is charge of electrons .

At the far left in Fig 3.1, the metal and the semiconductor are not in the contact and this system is not in thermal equilibrium. If they are brought into an intimate contact, there will be a net charge at the surface that causes an electric field[22]. Charges can move from the metal to the semiconductor, or vice versa, until electronic thermal equilibrium is established, as a result the Fermi-levels on both sides lining up and consequently bending of band comes out. If $\phi_m > \phi_s$, relative to the Fermi-level in the metal, the Fermi level in the semiconductor will be lowered by an amount equal to the difference between the work functions. This potential difference $q\phi_m - q(\chi + V_n)$ is called the contact potential. $q\chi$ is the electron affinity measured from the bottom of the conduction band to the vacuum level. As the distance δ decreases, an increase in the negative charge at the metal surface occurs. An equal and opposite charge (positive) must exist in the semiconductor. This causes the build up of charges on both sides of the interface, resulting in an electric field and therefore a potential gradient according to Poisson's equation $\frac{d^2V}{dx^2} = \rho(x)$. This is the so-called band bending. Because of the relatively low carriers concentration, this positive charge is distributed over a barrier region near the semiconductor surface. When δ is small

enough to be comparable with the interatomic distance, the gap becomes transparent to electrons, the electrons will move to the metal leaving positive charge carriers behind, as a result a depletion layer of width w will be created at the metal semiconductor interface (Fig.3.1). Hence we obtain the limiting case as shown in the far right.

It is clear that the limiting value of the barrier height $q\phi_{Bn}$ (neglecting the Schottky lowering), is given by

$$q\phi_{Bn} = q(\phi_m - \chi)$$

The barrier height is simply the difference between the metal work function and the electron affinity of the semiconductor. Moreover, the charge separation that cause the electric field will create a built in potential difference that varies with the width of the depletion region inside the space charge, hence the potential energy $\varphi(W)$ of the electrons increases and reaches its maximum value $\varphi(0) = qv_b$ at the metal-semiconductor interface.

The second limiting case is where a large density of surface state present on the semiconductor surface. When the metal-semiconductor is at equilibrium, the Fermi-level of the semiconductor relative to the metal must fall an amount equal to the contact potential and, as a result, an electric field is produced in the gap δ . If the density of the charge state is sufficiently large to accommodate any additional surface charges resulting from diminishing δ , without appreciably altering the occupation level E_F , the space charge in the semiconductor will remain unaffected. As a result the barrier height is determined by the property of the semiconductor surface and is independent of the metal work function.

If the work function of the metal is less than that of the n-type semiconductor, electron will transported from the metal to the semiconductor setting up a negative charge in the contact layer. In this case the energy of the electron $\varphi(W)$ decreases as it approaches the surface. This leads to an increase in the free charge carrier concentration inside the contact layer of the semiconductor and increase the conductivity. For this reason such a layer is ohmic, see Fig.3.2[20]

For an ideal contact between a metal and a p-type semiconductor, the barrier height,

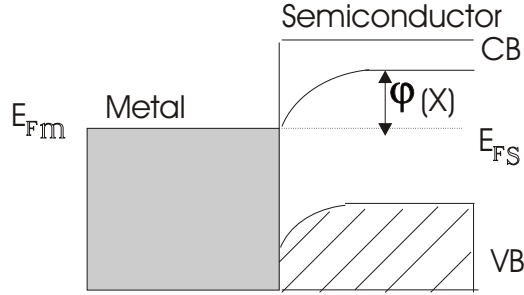


Figure 3.2: Band diagram for n-type semiconductor-metal contact with $\phi_m < \phi_s$

$q\phi_{Bp}$, is given by[23].

$$q\phi_{Bp} = E_g - q(\phi_m - \chi).$$

If the work function of metal is smaller than that of the p-type semiconductor a rectifying barrier will be formed at the interface. As a result, we obtain the band diagram shown in Fig.3.3a which represents ohmic contact. However, if $\phi_m < \phi_s$, this gives rise to rectification, Fig 3.3b.

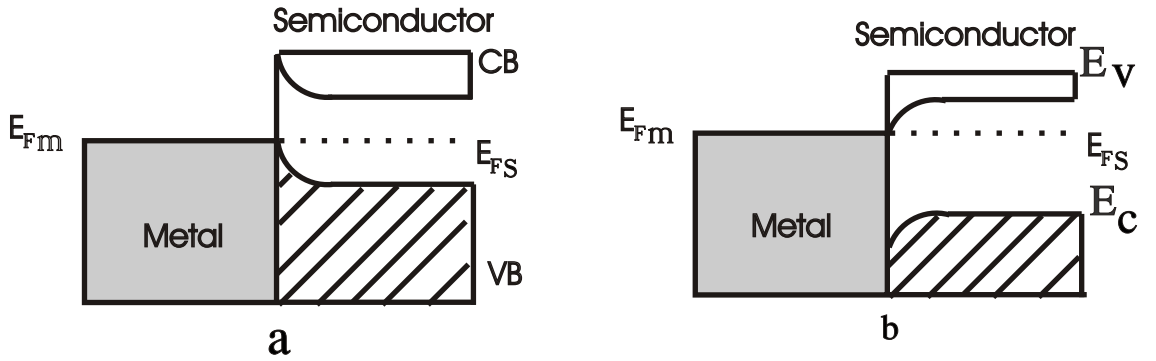


Figure 3.3: Band diagram for p-type semiconductor-metal contact for (a) $\phi_m > \phi_s$, which is ohmic and (b) $\phi_m < \phi_s$, which is rectifying

For a given semiconductor and for any metals, the sum of the barrier heights on the n-type and the p-type substrates is thus expected to be equal to the band gap, or

$$q(\phi_{Bp} + \phi_{Bn}) = E_g.$$

In general, the barrier height of a metal-semiconductor system are determined by both the metal work function and the surface states. A general expression of the barrier height

can be obtained on the basis of the following two assumptions : (1) with intimate contact between the metal and the semiconductor and with the interfacial layer of atomic dimension, this layer will be transparent to electrons and can withstand a potential difference across it, and (2) the surfaces per unit area per electron volt at the interface are a property of the semiconductor surface and is independent of the metal.

3.3 Current-Voltage Characteristics

The transport in the metal-semiconductor interface is due to majority carrier, in contrast to that in the p-n junction where the minority carriers are responsible for electrical transport. Across metal-semiconductor junction there are two mechanism by which the charge transport can occurs: (1) Drift, in which the motion of the charges is due to an external field (or potential), and (2) Diffusion, in which a current develops due to the difference in carrier concentrations in the materials. During the drifting case the direction of the the applied voltage (bias) determines the way of charge transfer. This can be described as follows. Whenever a metal and a semiconductor are in intimate contact, there exists a potential barrier between the two that prevents most charge carriers (electrons or holes) from passing from one to the other. That is, only a small number of carriers have enough energy to get over the barrier and cross to the other material. When a voltage is applied to the junction, it can have one of two effects: it can make the potential barrier lower or higher from the semiconductor side. The bias does not change the barrier height from the metal side. The result of this is a Schottky Barrier (rectifying contact), where the junction conducts for one bias polarity, but not the other. The applied voltage across the junction is a forward bias if it is positive and a reverse biased if the applied voltage is negative. The four basic sources of current under the forward bias are (a) emission of the carriers over the top of the barrier, (b) quantum mechanical tunnelling through the barrier, (c) recombination in the space charge region, (d) recombination in the neutral region [24]

According to the Thermionic emission theory (appendix A), the transport equation of an ideal metal/semiconductor rectifying contact is given by a Schottky barrier diode equation [23]

$$J = J_0 \left[\exp\left(\frac{qV}{nkT}\right) - 1 \right]$$

Where J is the total current density and J_0 is the value of the reverse saturation current density, q is the charge of the electron, V is the applied voltage, k is the Boltzmann's constant, T is the absolute temperature and n is the quality or ideality factor of the semiconductor. The value of J and J_0 determines the type of contact at the interface.

If $J_0 \ll J$, the contact will effectively block current flow for one sign of the applied voltage (the bias voltage) and will display an exponential increasing current when the bias voltage is of the opposite polarity (called the forward bias). Better rectification properties may be obtained for decreasing values of the reverse saturation current J_0 [1]. Then the above equation for the current density can be applicable to the rectifying diode.

If $J_0 \gg J$, the junction will readily pass current for both sign of the applied voltage. In this case if the exponential term in the expression for J is expanded one can get

$$V = \frac{nkT}{qJ_0} J$$

Which gives a linear and ohmic response displayed by the metal-semiconductor contact system.

If J is comparable to J_0 (neither of these extreme cases), the J-V characteristics is non ohmic and non rectifying, and the plot of J vs V will show a symmetric curve. If the function obeys the first condition, we can find J_0 by extrapolating the linear part of $\ln J - V$ plot to the $\ln J$ axis at small forward bias voltage . Once J_0 is determined we can find the barrier height from the relation

$$\phi_b = \frac{kT}{q} \ln \left(\frac{A^* T^2}{J_0} \right)$$

Where $A^* = 120AkT^2/cm^2$, see Appendix A, and the ideality or quality factor of the diode can be calculated from the relation

$$n = \frac{q}{kT \left(\frac{\partial \ln J}{\partial V} \right)}.$$

for Diodes $n \geq 1$

In the case of Metal-insulator-Metal (MIM) junction, the electron in the first metal can tunnel and/or thermionically enter into the insulator, and there can be collected by the second metal[23]. The expression for the current will be described by the WKB approximation. However, for the metal-semiconductor-metal junction, we can use the expression for the MS, since both contact are between metal and semiconductor. If the two metals have different work functions, the direction of motion of the charge carriers across the semiconductor depend on the value of the metals work functions. In this case if the work function of the semiconductor is between the work function of the two metals, electrons will move from the semiconductor to the metal with lower work function and holes will move to the metal with the higher work function, provided that the semiconductor is p-type. The opposite takes place of the semiconductor is n-type. In the case of p-type, as discussed in the last subsection, the contact between the the metal with higher work function is ohmic and the one with the lower is rectifying.

The formation of the depletion region between the low work function metal and the polymer will act as a capacitor. The capacitance C of the depilation layer (see Fig. 3.1) with thickness W of the revers-biased semiconductor is given by [1]

$$\frac{1}{C^2} = \frac{2}{qA_s^2\epsilon_s N_d} \left[\phi_b - V_n - V - \frac{kT}{q} \right]$$

where A_s is the cross-sectional area of the device, ϵ_s is the dielectric constant of the semiconductor, N_d is the homogeneous dopant density, V is the applied voltage, $\frac{kT}{q}$ is the thermal energy expressed in volt. The other quantities are as defined in Fig 3.1.

3.4 Impedance spectroscopy and circuit models

Impedance is an important parameter used to characterize electronic circuits, electric components, and the materials used to make components. Impedance (Z) is generally defined as the total opposition a device offers to an alternating electric current (AC) at a given frequency, and can be represented graphically as a complex quantity on a vector

plane. An impedance vector consists of a real part (the resistance R) and an imaginary part (the reactance X) as shown in Figure 3.4a. Impedance can be expressed using the rectangular-coordinate form $R+jX$, or in the polar form as a magnitude and phase angle: $|Z| < \theta$.

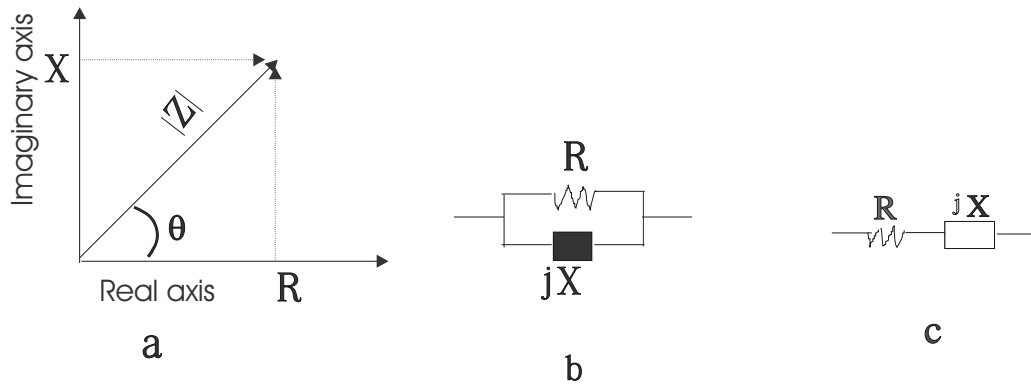


Figure 3.4: (a) Impedance Complex plane, (b) Parallel, (c) series connection of R, X

The mathematical relationship between R, X, $|Z|$ and θ can be shown as

$$Z = R + jX$$

$$Re(Z) = R = |Z| \cos \theta$$

$$Im(Z) = X = |Z| \sin \theta$$

$$|Z| = \sqrt{R^2 + X^2}$$

$$\theta = \tan^{-1} \frac{X}{R}$$

In some cases, using the reciprocal of impedance is mathematically expedient. In which case $1/Z = 1/(R+jX) = Y = G+jB$, where Y represents admittance, G conductance, and B susceptance. Impedance is a commonly used parameter and is especially useful for representing a series connection of resistance and reactance, because it can be expressed simply as a sum, R and X. For a parallel connection, it is better to use admittance (see Figure 3.4b and c)[26].

Impedance spectroscopy is a power full method of characterizing many of the electrical properties materials. It can be used to investigate the dynamics of bound or mobile charge

in the bulk or interfacial regions of any type of material that is ionic, semiconducting, mixed electronic-ionic or even insulating[1]. The general approach is to apply an electrical stimulus such as a known voltage or current of a known frequency to the device under test (DUT) and observe the resulting current and voltage response. The common approach is to apply a voltage to the electrodes on either side interface and measure the amplitude and the phase shift of the resulting current. Impedance spectroscopy has been used to study the electrical and dielectric properties of polymers[18, 19]. From this technique we can find the resistance (R) and capacitance (C) of junction in the DUT.

The real and the imaginary parts of the impedance are recorded as a function of frequency and plotted on the complex plane. The real part is plotted along the x-axis and the negative of the imaginary part along the y-axis. Ideally the imaginary part of the impedance is zero at frequency, $\omega = 0$ and ω approach ∞ [17]. This plot forms a semicircle with the center on the real axis. The very important idea in the modelling studies is to match the experimental results with the impedance of an ideal equivalent circuit consisting of resistance and capacitance[6].

The main purpose of this section to show by observing the impedance response of our sample, we are able to model its equivalent electric circuit. In the modelling one seeks to match the experimental impedance with the equivalent circuit composed of ideal resistances and capacitors. In the circuit the resistance (R) is taken to represent the dissipative component of the electric response, and the capacitance (C) describes the storage component of the electric material. Resistance and capacitance can be combined in a variety of forms, leading to a array of phenomenological models that can describe varies combinations of polarization mechanisms in dielectric materials.

Consider that there is a circuit with R and C connected in parallel. Moreover, assume that the applied voltage and its response current are sinusoidal in nature with frequency $\omega = 2\pi f$ and

$$I = \frac{d(CV)}{dt} = \omega CV_0(j \cos \omega t - \sin \omega t)$$

Hence, the impedance of the circuit can be expressed as follows.

From capacitive reactance X_c , which is defined as the ratio of $V(t)$ to $I(t)$,

$$X_c = \frac{V_0(\cos \omega t + j \sin \omega t)}{\omega C V_0(j \cos \omega t - \sin \omega t)}.$$

After normalization, we obtain

$$X_c = \frac{1}{j\omega C}.$$

From the impedance of R and C in parallel, Fig 3.5

$$Z = \left(\frac{R}{1 + jR\omega C} \right) = \frac{R}{1 + jR\omega C} \left(\frac{1 - jRC\omega}{1 - jRC\omega} \right).$$

But RC is defined as the relaxation time τ , therefore,

$$Z = \left(\frac{R}{1 + \tau^2\omega^2} \right) - j \frac{R\tau\omega}{1 + \tau^2\omega^2}.$$

Hence the real and the imaginary component of the impedance will be

$$\begin{aligned} \operatorname{Re}(Z) &= \frac{R}{1 + \tau^2\omega^2} \\ -\operatorname{Im}(Z) &= \left(\frac{R\omega\tau}{1 + \tau^2\omega^2} \right). \end{aligned}$$

But from elementary geometry $\omega\tau = \tan \theta$, where θ is the phase difference between the voltage and the current. $\theta = 0$ for pure resistance and $\theta = \frac{\pi}{2}$ for pure capacitance. The combination of resistance and capacitance in a network will have $0 < \theta < \frac{\pi}{2}$

Hence,

$$\operatorname{Re}(Z) = R \cos^2 \theta$$

and

$$\operatorname{Im}(Z) = R \cos \theta \sin \theta$$

Using a trigonometric identity ($\cos^2 \theta = \frac{1 + \cos 2\theta}{2}$ and $\cos 2\theta = 2 \sin \theta \cos \theta$)

$$\begin{aligned} \operatorname{Im}(Z) &= -\frac{R}{2} \sin 2\theta \\ \operatorname{Re}(Z) &= \frac{R}{2} [1 + \cos 2\theta] \end{aligned}$$

From this it is seen that the imaginary component is maximum when $\sin 2\theta$ is maximum, that is at $2\theta = \frac{\pi}{2}$, in which case $-Im(Z) = \frac{R}{2}$ and $\omega\tau = 1$. Then the diameter of the semicircle corresponds to R . The Cole-Cole plot of this circuit will be a semicircle whose center lies on the real axis of the impedance[25]. If we add a resistance R_c in series to the

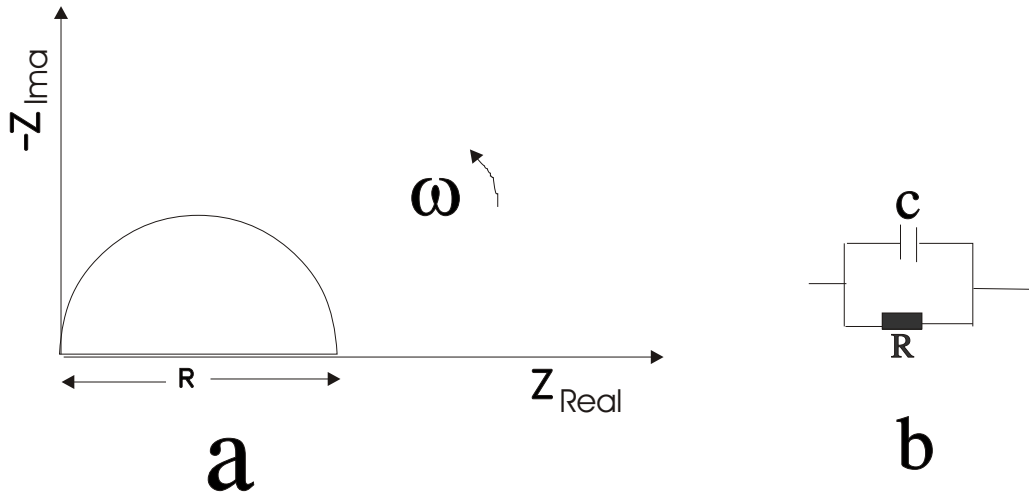


Figure 3.5: Representation of (a) Z of the RC circuit in complex plane and (b) RC connected in a parallel arrangement

above modelling the impedance will be given by

$$Z = R_c + \frac{R}{1 + j\omega C}$$

Such a combination is an equivalent circuit model for a junction between a metal and a semiconductor and the depletion region accounts for the capacitance C and resistance R , and R_c accounts for the observed contact resistance[18]

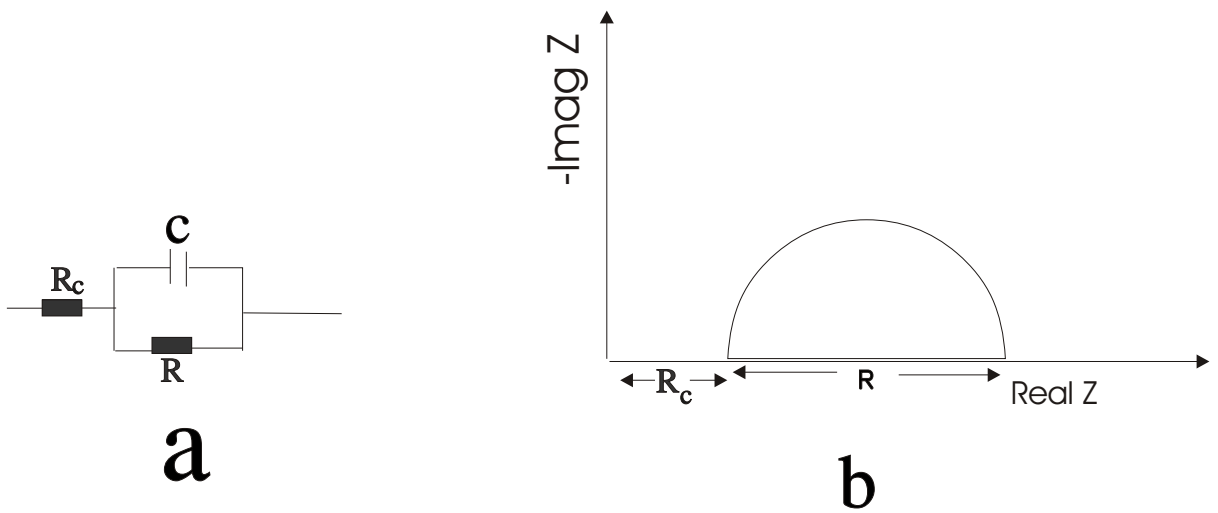


Figure 3.6: (a) Combination of resistance R_c , R and capacitance C , (b) Cole-Cole drawing of the impedance Z of the circuit.

Chapter 4

Sample Preparation and Procedures Used

4.1 Forming ITO/Polymer/Al sandwich

Commercially available Indium Tin oxide (ITO) coated transparent glass was used in the device preparation. The glass was cut with rectangular dimension, 2.5cm by 1.5cm. About half of the ITO was etched using magnesium (Mg) and concentrated hydrochloric acid (HCl) solution, by covering the part not to be etched with tape. To etch the substrate, HCl was prepared in a cleaned beaker and the half covered substrate was placed with the ITO coated side facing the HCl, so that the hydrogen that evolves from the reaction with Mg and HCl will directly attack the ITO. Then strips of Magnesium was added to the HCl. This technique of etching is simple and effective. After etching the substrate was washed for about 5min with distilled water, followed by washing with Acetone for about 15min and rinsed in Ethanol respectively.

The polymer (MDMO-PPV) was prepared in the form of solution using dichlorobenzene as a solvent. One form of the solution was pure polymer and the other one had fullerene (C_{60}) included in it. To prepare the polymer solution without fullerene 5mg MDMO-PPV polymer powder was dissolved in 1ml of dichlorobenzene solvent. The fullerene

containing polymer based solution was prepared in 1ml solvent with 1:1Wt% ratio of fullerene mixture (5mg each). Then films of, MDMO-PPV, and MDMO-PPV+ C_{60} were deposited on different ITO-coated glass electrodes by drop casting. This drop casting technique was preferred compared with the spin coating due the nature (ball shaped) (see Fig 4.2) of the mixture (C_{60}) that can roll out during the high speed spinning. Moreover, since drop casting is made by hand it is possible to make the polymer layer more thick so that the probability that the aluminium can make contact during deposition is small. For the pure polymer sample both the spin coating and drop casting technique were used. The one prepared with spin coated was very thin and uniform. All the spin coated processes were done using a programmable spinner system at a speed of 600rev/min. In both methods the polymer covers the whole area of the sample, so for electrical contact parts of the polymer was removed (on both edges) with dichlorobenzene. Finally the Aluminium was deposited on the polymer side in a vacuum about (10^{-5} mbr) using Edwards Auto 306 vacuum evaporator. In this way the Al/MDMO-PPV/ITO and Al/(MDMO-PPV+ C_{60})/ITO sandwich structure on several glasses were prepared. (see Fig.4.1)

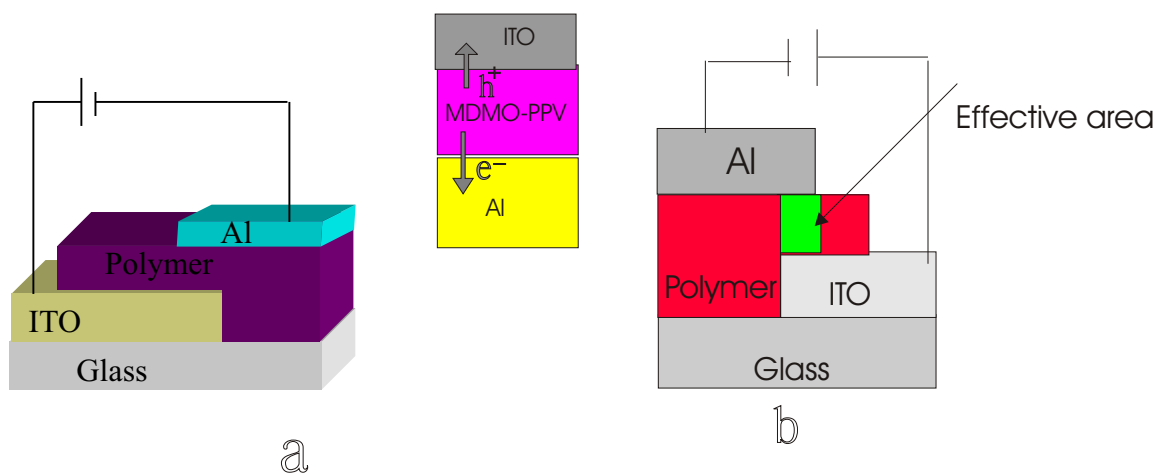


Figure 4.1: (a) Three-dimensional view with the way charge transfer across the sample, (b) Side view showing effective area.

The effective area of the junction (the area under the contact of Al, polymer and ITO (see

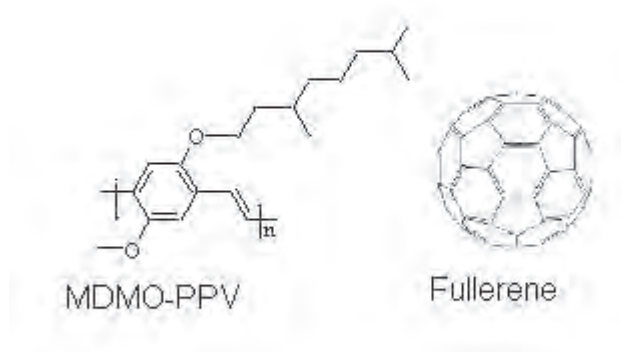


Figure 4.2: Chemical structure of MDMO-PPV and C₆₀

Fig.4.1b)) of the device was about $4 \times 10^{-2} \text{ cm}^2$. The sandwiched structure shown in Fig.4.1 provides a means to measure the current-voltage and complex impedance spectroscopy.

4.2 Measurement Techniques

Absorption Measurement

The optical absorption spectrum of MDMO-PPV and MDMO-PPV/C₆₀ were taken after the solution of both samples was spin coated and hand casted on different glass substrate, with smooth and uniform distribution in the case of spin coating, using PERKIN-ELMER UV/VIS/NIR λ -19 spectrometry. This spectra measurement is used to calculate the band gap of the polymer under test by using the relation[4]

$$E_g = h\nu = \frac{hc}{\lambda}$$

where $h = 6.625 \times 10^{-34} \text{ J/sec}$ is Plank's constant and $c = 3 \times 10^8 \text{ m/sec}$ and λ is the wave length at which the absorption curve starts to bend upward. The measurement of this spectrum also shows the wavelength at which the maximum absorption takes place. If the sample under test absorbs in the visible range wavelength that would be one criteria for

the material to serve for solar cell application. For both pure MDMO-PPV and blended with fullerene the spectrum measurement are shown in Fig.5.1 and 5.2.

Current-Voltage Measurement

To determine the current density-voltage characteristics of the sample the current-voltage characteristics of the diodes were measured by using HP 4140 B PA Meter/DC voltage source, together with HP 16055A-TEST FIXTURE. During the measurement, the samples were at room temperature (about 25°C), dry air and in a dark environment. The DUT was connected in such a way that the applied voltage supports the motion of the charge carrier. i.e. the aluminum is connected to "high", i.e, the negative terminal, and, the ITO side to V_A (positive terminal). The applied voltage was scanned between -3V to 3V in step of 0.25V for both samples. As the value of the applied voltage was increased the nature of the I-V curve did not change except for the fact that at extreme voltage amplitude the current amplitude gets large. The data were taken point by point with 1sec interval, which is fixed by the instrument using the "data points" and "step delay" keys on the PA DC voltage source. Finally, the current density was calculated by dividing the current value by the effective area of the diode (the sample area), and the plots of J-V and $\ln J$ -V for both blended and pure are shown in section 5.2.

Impedance Measurement

Complex impedance spectroscopy of the DUT was measured as a function of frequency and applied voltage using HP 4192A LF Impedance Analyzer together with HP 10047A-TEST FIXTURE. The Cole-Cole plot for Al/MDMO-PPV/ITO and Al/MDMO-PPV/ C_{60} /ITO are shown in the following chapter. In both DUT's the data were taken for a frequency range between 0.5kHz to 100kHz in step of 10kHz for a bias voltage of ± 3 , ± 2 , ± 1 . For additional values of the frequency, both the real and the imaginary values were measured, and the minimum values were found for the frequency at about 100kHz. For every applied voltage a sinusoidally oscillating voltage of $V_{rms} = 20\text{mV}$ was used and the zero offset were done at a spot frequency of 100kHz. In order not to disturb the contact resistance, the offset were done only once for one measurement of the all biased voltage.

Chapter 5

Results and Discussion

5.1 Absorption Measurement

The optical absorption of both Al/MDMO-PPV/ITO and Al/MDMO-PPV/ C_{60} /ITO (Fig. 5.1 and 5.2) sandwich sample were measured. The data indicates that absorption of Electromagnetic radiation occurred in the visible range. The spectrum of pure MDMO-

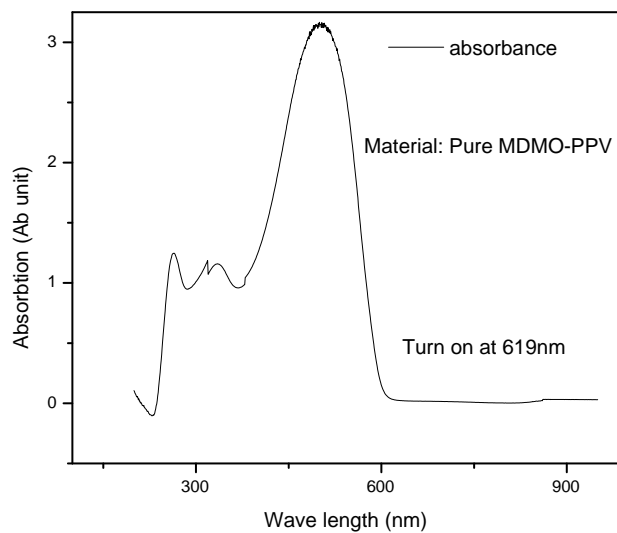


Figure 5.1: *Absorption spectrum of Pure MDMO-PPV*

PPV shows that absorption started nearly at wave length of 619nm, which corresponds to an energy band gap of 2.0023eV. From the fact that the energy band gap for most semiconductors falls in the range between 0.7eV and 3eV, MDMO-PPV can be categorized as a semiconducting organic polymer.

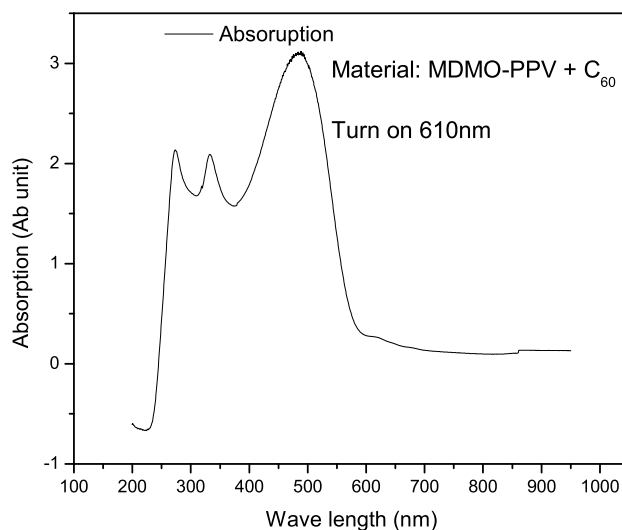


Figure 5.2: Absorption spectrum of MDMO-PPV blended with C_{60}

On the other hand, widening of the absorption region and a shift of the start of the absorption curve peak was observed for the fullerene blended polymer (see Fig.5.3). The shift of absorption point could be as a result of the superposition of the absorption lines of the polymer and fullerene. The non linear intensity variation of the C_{60} absorption line that is superposed with MDMO-PPV results in the peak shift from the maximum as seen in Fig 5.3. Moreover, it can also be due to the interaction of the polymer with the fullerene at the ground state.

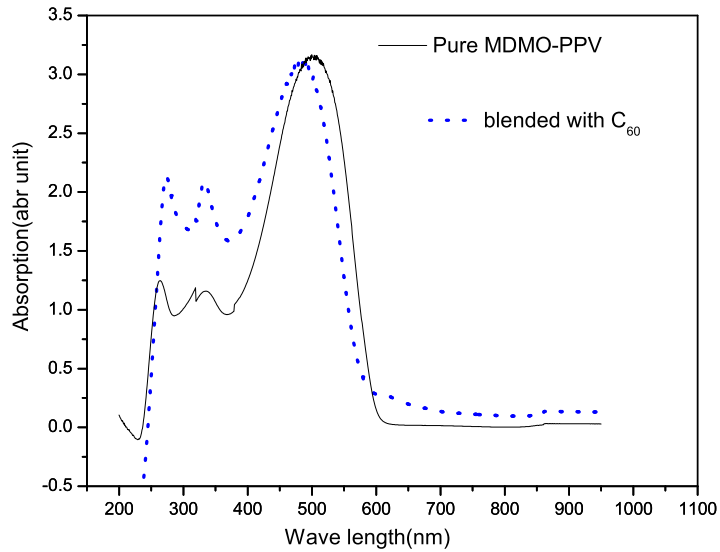


Figure 5.3: Absorption spectrum of pure MDMO-PPV and blended with C_{60}

5.2 Current-Voltage Characteristics

The I-V curve of Al/(MDMO-PPV= C_{60})/ITO sandwich structure in the dark is asymmetric and non-ohmic, see Fig.5.4 through 5.7. Under forward bias, which corresponds to positive voltage applied to the ITO electrode, the current increased fast, whereas in the reverse direction the current was almost blocked (Fig.5.4). This confirms the formation of a Schottky barrier at the interface between aluminium and the polymer. According to the theory of the Schottky barrier, a rectifying contact could be formed at the interface whenever the work function of metal is smaller than that of p-type semiconductor, and an ohmic contact formed if the work function is greater than that of the semiconductor. See Fig.3.4b. If the work function were in the reverse order, an ohmic contact would be created rather than a rectifying on which allows the current to vary linearly with the applied voltage across the junction (Fig 3.3 a). In all cases the interface between the aluminum and polymer is rectifying and the polymer and ITO junction is ohmic. Hence, the polymer MDMO-PPV is a p-type semiconductor whose work function is between that of aluminium (4.25eV) and ITO (4.85eV). When we look at the graph of the current density

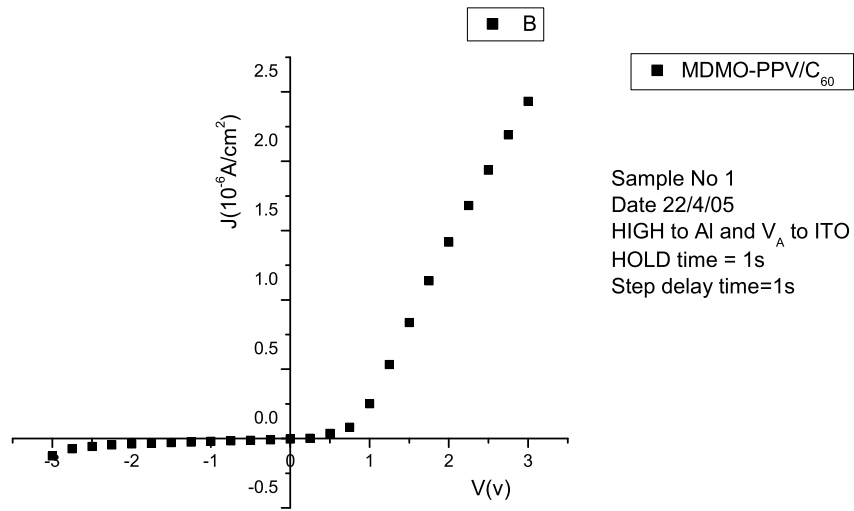


Figure 5.4: Current density J Vs applied voltage for MDMO-PPV blended with C_{60}

verses the applied voltage, there is an exponential increasing current for a forward voltage. From the curve it is clear that the device shows rectification property with a rectification ratio of about 10^2 in the dark with a turn on voltage at about 1V (Fig 5.4).

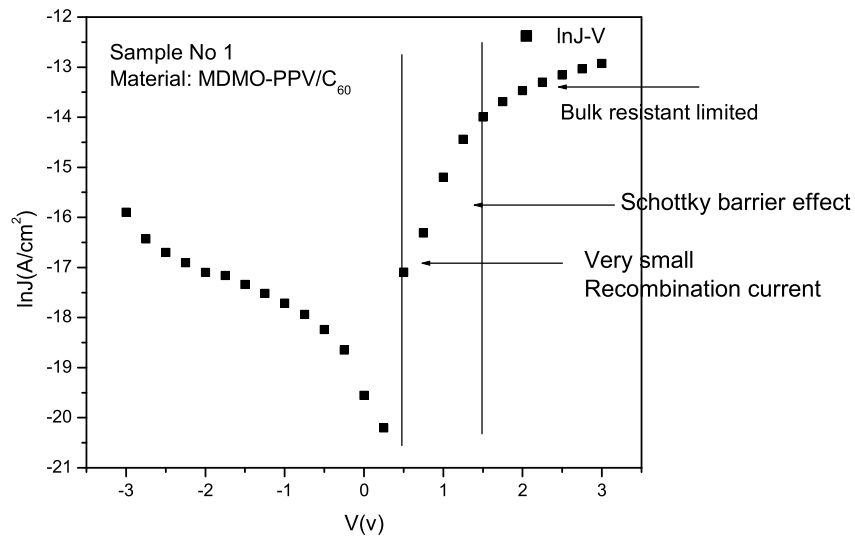


Figure 5.5: The logarithm of current density J Vs applied voltage MDMO-PPV blended with C_{60}

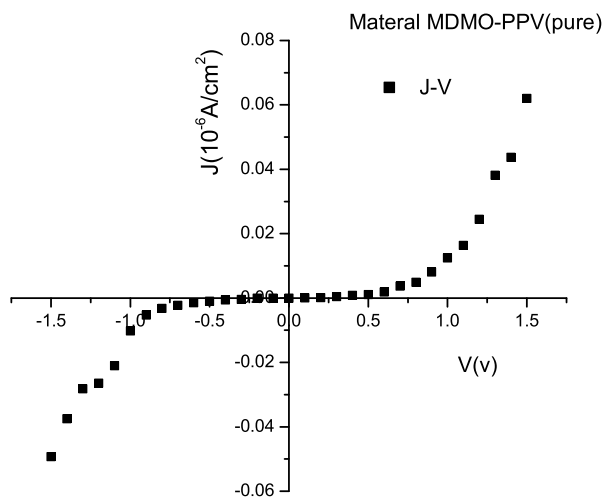


Figure 5.6: *Current density Vs applied voltage for pure MDMO-PPV*

A semi-logarithmic plot of the current density (J) versus the applied voltage is shown in Fig.5.5. It shows two regions in the forward direction. From about $0.3V < V < 1.9V$ the current is an exponentially increasing, showing the formation of depletion layer between aluminum and the polymer. The second region is for $V \geq 1.9V$. When the applied voltage increases beyond this value the current is almost linear, showing that the bulk resistance of the polymer limits further enhanced transfer of charges. These regions also show the non existence of the recombination current for the case of fullerene blended polymer. The absence of the recombination current in this case is due to the presence of the fullerene. Comparison of Figure 5.5 and 5.7 shows that there is small recombining current inside the depletion region in the case of Fig 5.7 (pure MDMO-PPV). On the other hand it is almost non-existent in the case of MDMO-PPV blended with fullerene. One of the main objective of this thesis is to see the influence of the fullerene when blended with the polymer. When conducting polymers are mixed with an electron acceptor or donor, their conductivity should be enhanced. Comparison between pure MDMO-PPV and with that of blended of fullerene (MDMO-PPV C_{60}) (Fig 5.6) shows, there is large current value in the case of Fullerene blended polymer (Fig 5.4) for the same bias voltage, showing that

the conductivity has enhanced.

From the very nature of fullerene which is high electron acceptor in the polymer, it plays a significant role in collecting (trapping) the free charge carriers created in the depletion region by preventing them from recombination. As a consequence, large amount of current is recorded in the same range of bias voltage.

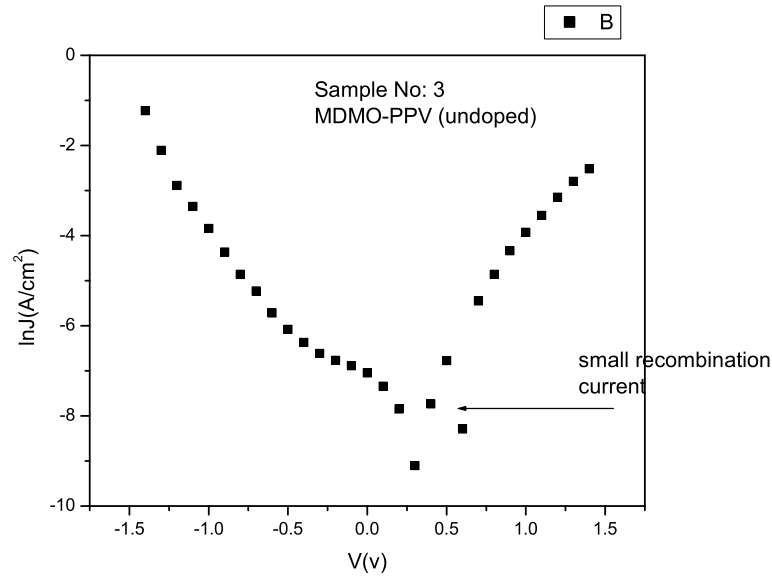


Figure 5.7: *Logarithm of Current density Vs applied voltage for pure MDMO-PPV*

On the other hand, the semi-logarithms graph tells us about certain properties of the DUT. For instance, by extrapolating the straight line portion of the curve $\log J$ vs V (Fig 5.5 and 5.7) for small positive voltage, usually close to $V = 0V$ (Fig 5.8 and 5.9), one can find the values for the reverse saturation current. From both graphs, the reverse saturation current is determined to be about $9.81 \times 10^{-18} A/cm^2$ for the fullerene blended polymer while it is $1 \times 10^{-9} A/cm^2$ for the pure MDMO-PPV polymer.

Once J_0 is found, we can find the barrier height per unit charge using the relation

$$\phi_b = \frac{kT}{q} \ln \left(\frac{A^* T^2}{J_0} \right)$$

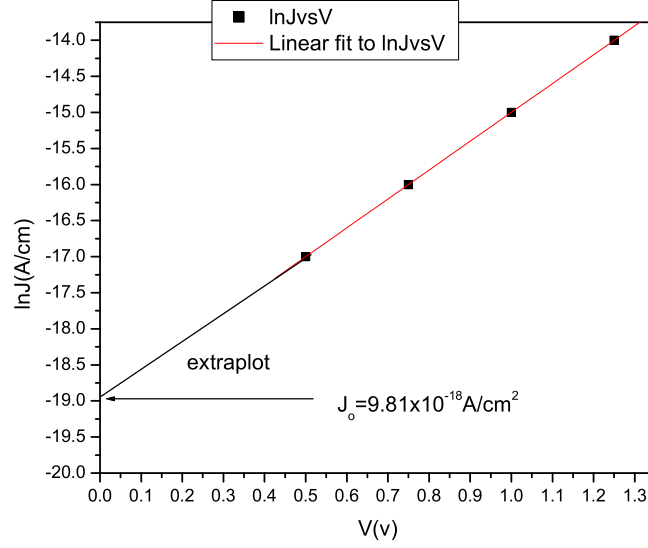


Figure 5.8: Linear part of $\ln J$ vs V curve for $Al/MDMO-PPV/C_{60}ITO$

where

$$K = 8.62 \times 10^{-5} eV$$

$$T = 295^0 K$$

$$A = 120 \frac{A}{cm^2 K^2}.$$

Using this relation, the barrier height is found to be 1.43eV for the fullerene blended polymer and 0.95eV for the pure MDMO-PPV polymer. Such difference in the values of the reverse saturation current J_o , in the reverse voltage region, suggests that the current will be blocked by large potential barrier of the fullerene blended polymer while the current is relatively less prevented for the reverse applied voltage in the case of pure MDMO-PPV polymer. A small reverse saturation current J_o is the property of well rectifying polymer. On the other hand, from the slope $(\frac{\Delta \ln J}{\Delta V})$ of the graph (Fig 5.8 and 5.9), the ideality or quality factor n can be calculated using the relation

$$n = \frac{q}{kT \left(\frac{\partial \ln J}{\partial V} \right)}.$$

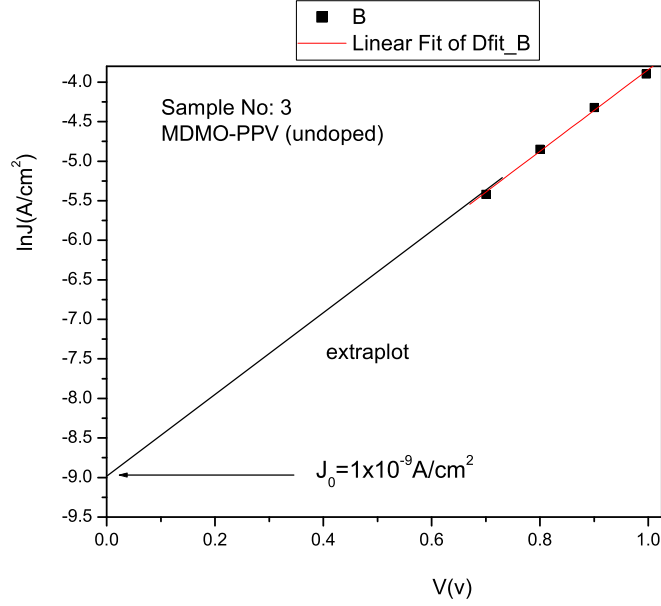


Figure 5.9: Linear part of $\ln J$ vs V curve for Al/MDMO-PPV/ITO

With the slope about 6.12 for the fullerene blended polymer and 5.06 for the pure MDMO-PPV polymer, and the other values as defined before, the ideality factor for the pure MDMO-PPV polymer and the fullerene blended are found to be 6.42 and 7.8 respectively. Theoretically, ideality factor should be greater than or equal to unity.

There are also additional terms that can describe the DUT. These are the short circuit current I_{sc} , and the open circuit voltage V_{oc} , etc. In this experimental work we found values of I_{sc} and V_{oc} from the current-voltage measurement and there values are as summarized in table 5.1 and 5.2 below. The short circuit current is the current when the voltage is

$J_0(A/cm^2)$	$\phi_b(ev)$	n	I_{sc}	V_{oc}
9.81×10^{-18}	1.43	6.42	129nA	250mv

Table 5.1: Electrical character of MDMO-PPV blended with fullerene

zero. It is found to be 129nA for MDMO-PPV/ C_{60} and 180nA for MDMO-PPV.

The open-circuit voltage is the voltage when the current is approximately zero. It was found to be 250mV for MDMO-PPV/ C_{60} and 200mV for MDMO-PPV.

$J_0(A/cm^2)$	$\phi_b(ev)$	n	I_{sc}	V_{oc}
1×10^{-9}	0.97	7.8	180nA	200mv

Table 5.2: Electrical character of pure MDMO-PPV

5.3 Impedance Characteristics

Information about the bulk resistance and the Schottky diode can be obtained from complex impedance measurements. Fig 5.10 and 5.11 shows the Cole-Cole plot of the result of the impedance measurement for the applied biased voltage and frequency in the forward and reverse direction for both the MDMO-PPV polymer and the MDMO-PPV/ C_{60} polymer coated sample, respectively. The points in the figures are the measured coordinates of the real and imaginary components of the impedance. It can be clearly

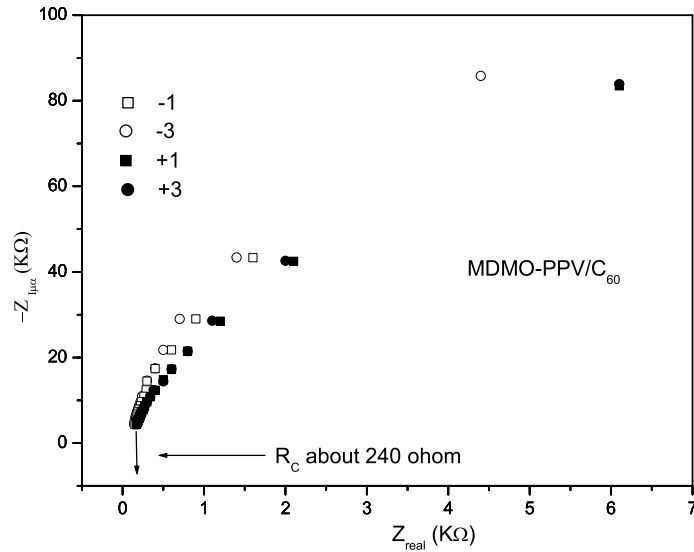


Figure 5.10: Cole-cole plot of Al/MDMO-PPV/ C_{60} /ITO

seen from the graphs, that the impedance spectra consists of a portion of a single semicircle whose diameter corresponds to the resistance of the depletion region for the respective bias voltage. These semicircles are bias voltage dependent the smaller the bias voltage is, the larger the diameter becomes (see Fig 5.10 and 5.11). This suggest that for smaller

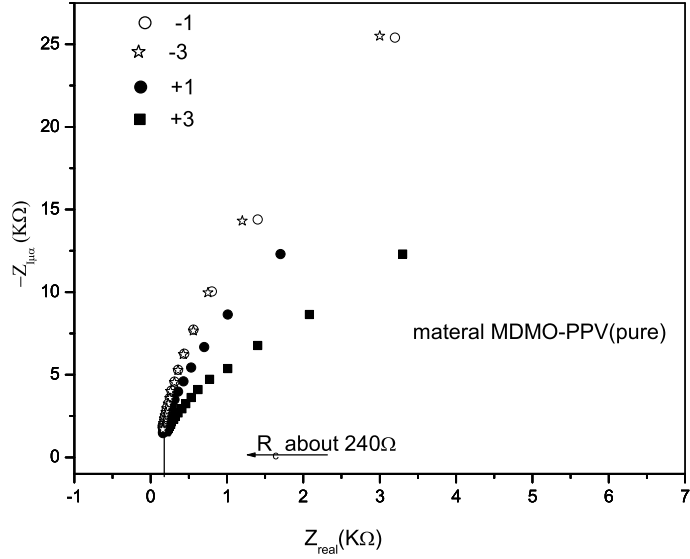


Figure 5.11: *Cole-cole plot of Al/MDMO-PPV/ITO*

biased voltages the resistance of the sample gets larger and current is reduced. The large radius for the reverse bias voltage clearly indicates that the current encounters greater resistance in the model compared with the forward bias mode. This result is consistent with the J-V curve discussed in the last section (Fig. 5.4). i.e., the current is blocked for the reverse applied voltage. It shows that the sample is resistive for the current in the reverse bias applied voltage, and the resistance decreases as we go from larger bias voltage to smaller (larger for smaller negative applied voltage). The two figures also show that the semicircle is displaced from the origin by a specific amount, giving the magnitude of the contact resistance of the sample. We can thus model the sandwich structure of the Al/MDMO-PPV/ C_{60} /ITO sample and the Al/MDMO-PPV/ITO sample by one parallel RC circuit in series with a contact resistance, R_C as shown below. In addition to these results, the measurement shows that, the value of the imaginary component comes closer to zero for smaller and larger value of frequency. As a result the full semicircle can be observed. However, the diameter of the semicircle can also be extrapolated from the available data. From the present measurement the contact resistance is determined to be 240Ω . The electric parameters like contact resistance (bulk resistance of the sample and

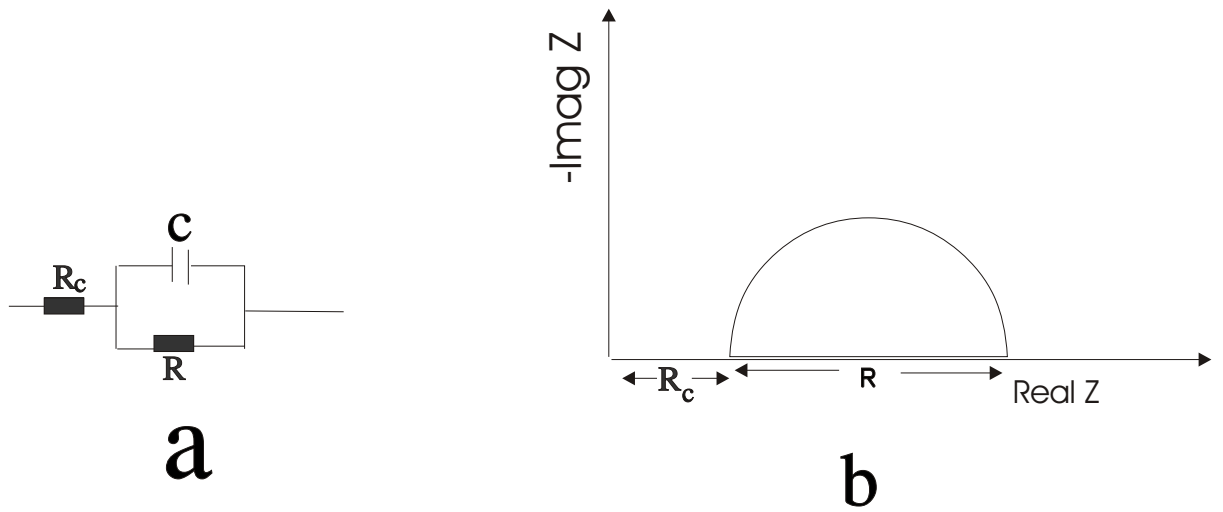


Figure 5.12: Model of Al/MDMO-PPV/C₆₀/ITO

$V_b(V)$	$R_c(k\Omega)$	$R_D(k\Omega)$	$C(\frac{nF}{cm^2})$
3	240	11	2.67
1	240	11.2	2.48
-3	240	12	2.26
-1	240	12.1	2.09

Table 5.3: Electrical characteristics collected from cole-cole plot of MDMO-PPV blended with fullerene that of ITO) , resistance of the depletion layer and the capacitance of the device for both samples are summarized in the table below (see also Fig 5.13 and 5.14).

To find the resistance of the depletion layer a circular fit to the complex impedance representation was performed with the help of "Origin soft ware" and estimates of the capacitance of the device for the corresponding bias voltage the relation $-Z_{ima} = \frac{1}{C\omega}$. $\omega = 2\pi f$ at the highest value of Z_{ima} was used. The values collected from impedance spectroscopy are summarized in table 5.3 and 5.4.

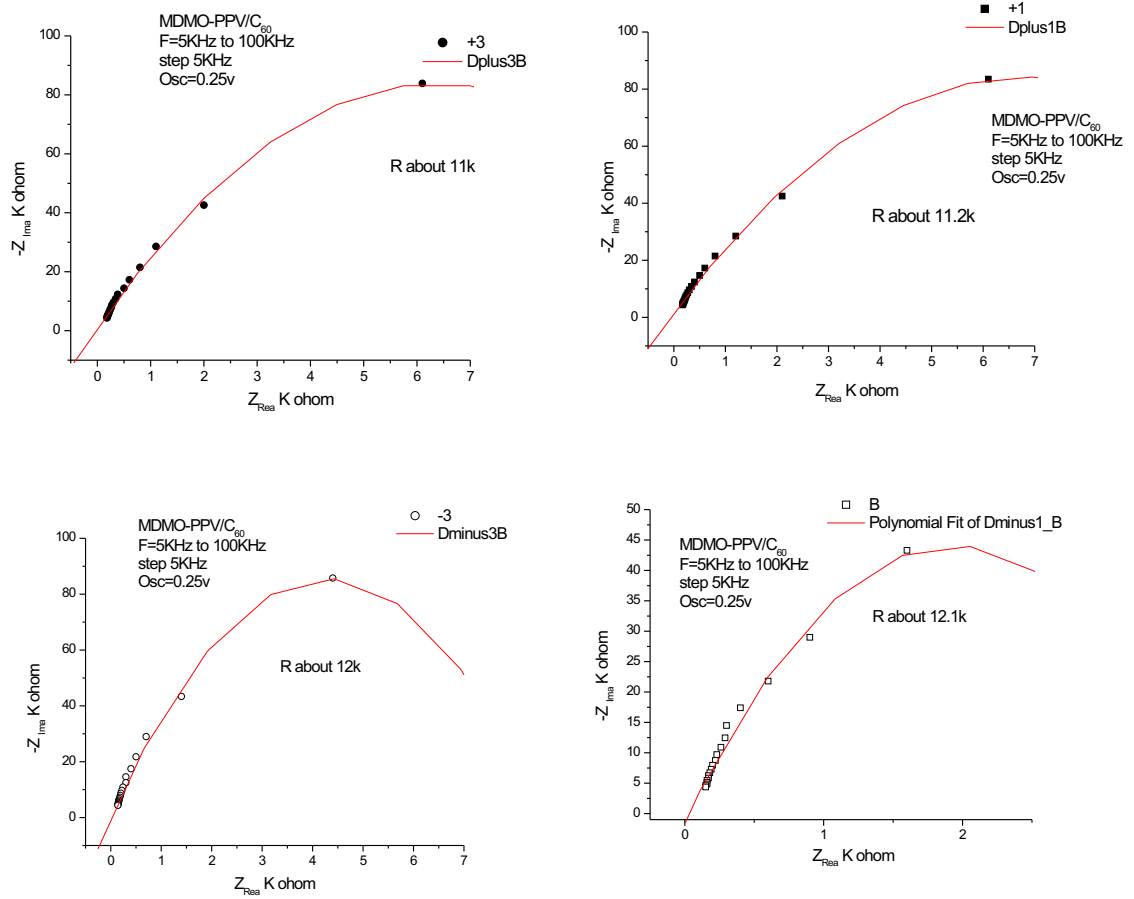


Figure 5.13: Extrapolate for Cole-cole plot of Al/MDMO-PPV/C₆₀/ITO

$V_b(V)$	$R_c(k\Omega)$	$R_D(k\Omega)$	$C(\frac{nF}{cm^2})$
3	240	6.4	0.191
1	240	8	0.191
-3	240	9.7	0.185
-1	240	10	0.1848

Table 5.4: Electrical characteristics collected from cole-cole plot for pure MDMO-PPV

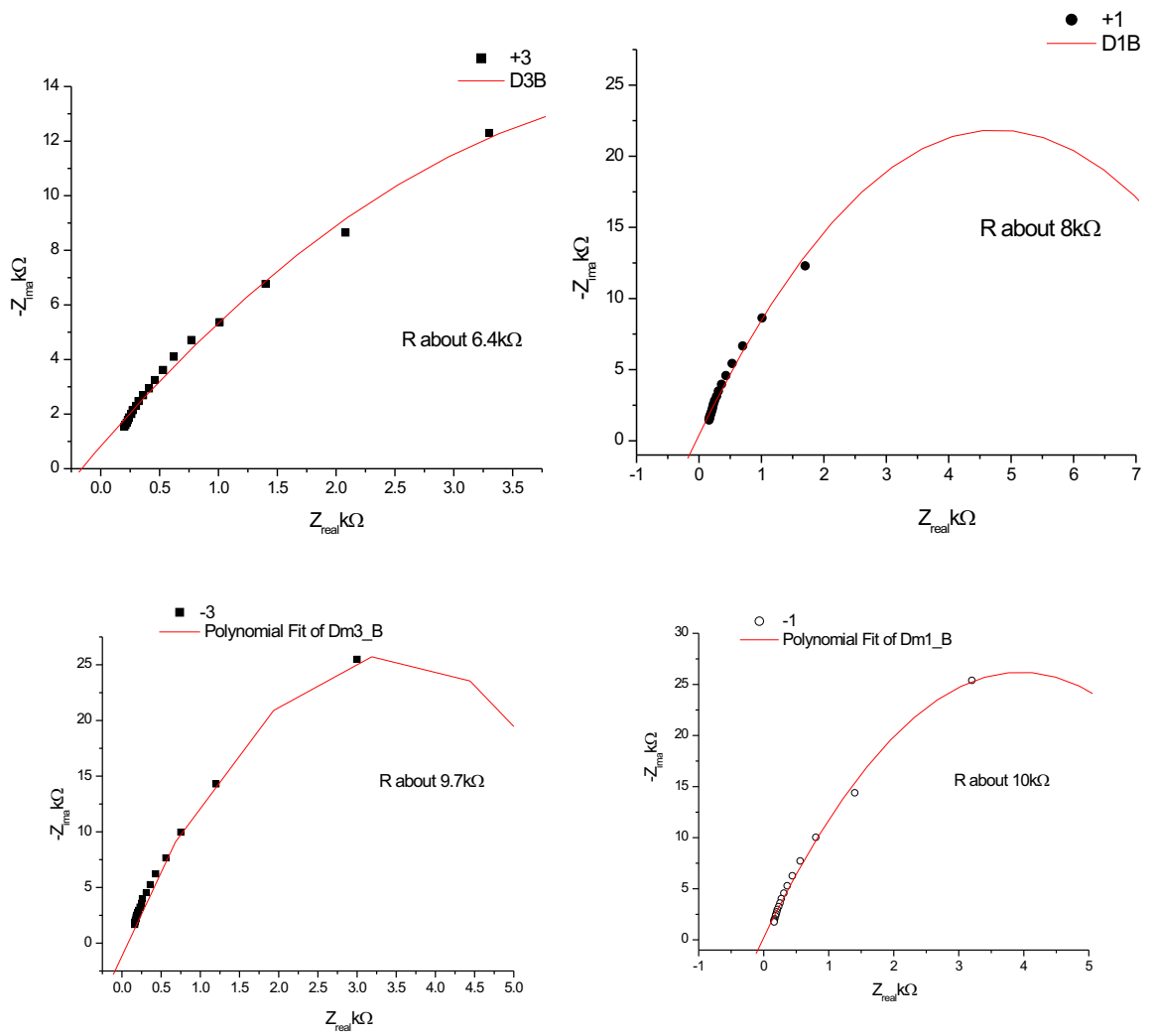


Figure 5.14: Extrapolate for Cole-cole plot of Al/MDMO-PPV/ITO

Conclusions

In this research, we studied the electrical property of the junction between Aluminum and conjugated polymer interface. The analysis of the study was based on various types of experimental results such as I-V characteristics and complex impedance measurement of the Al/MDMO-PPV/ITO and Al/MDMO-PPV/ C_{60} /ITO sandwich structures. Moreover, Electromagnetical absorption were taken from these polymers in order to determine energy band gap. The results show that the energy gap of the pure MDMO-PPV is 2.0023eV. In the literature, the energy band gap of MDMO-PPV range between 2eV to 2.3eV. Hence, our result is in good agreement with the report.

The Thermionic emission theory model has been applied to interpret the J-V characteristics of the diode junction. The I-V characteristics of both diodes junctions suggests that a Schottky barrier type junction is formed at the metal/semiconductor contact. The blended diode is found to be better rectifying than the the pure MDMO-PPV case. The use of fullerene in the mixture enhanced the diode quality. The quality factor of the diode is larger in the case of pure polymer due to trapping and recombination. The rectification ratio are about 100 for the C_{60} blended case and about 10 to 20 in the case of pure diode with quality factor 6.42 and 7.8, respectively.

The complex impedance curve at different bias voltages shows that the impedance of the depletion region at revers bias voltage is larger than the impedance of the corresponding forward bias voltage. This is consistent with the rectification behavior observed from the I-V characteristics. The Cole-Cole plot show that the the result exhibits a typical diode behavior representing metal semiconductor interface.

In general, for better diode characteristics this polymer can be blended with an electron acceptor, and it can be recommended for practical application, like use as a photovoltaic.

Appendix A

Thermionic Emission Theory

The Thermionic emission theory is derived from the assumption that (1) the barrier height ϕ_{Bn} is larger than kT , (2) electron collision with in the depletion region are neglected, and (3) the effect of the image charge is also neglected. Because of the above assumption the shape of the barrier profile is immaterial and the current flow depends solely on the barrier height . The current density $J_{s \rightarrow m}$ from the semiconductor to the metal is then given by the standard Thermionic emission equation

$$J_{s \rightarrow m} = \frac{qn(m^*)^{\frac{3}{2}}}{(2\pi kT)^{\frac{3}{2}}} \int_{-\infty}^{\infty} dv_y \int_{-\infty}^{\infty} dv_z \int_{v_{ox}}^{\infty} \exp\left[-\frac{m^*(V_x^2 + V_y^2 + V_z^2)}{2kT}\right] dv_x \quad (\text{A.1})$$

$$= qn \left(\frac{m^*}{2\pi kT}\right)^{\frac{1}{2}} \int_{v_{ox}}^{\infty} \exp\left(-\frac{m^*V_x^2}{2kT}\right) dv_x \quad (\text{A.2})$$

$$= qn \left(\frac{kT}{2\pi m^*}\right)^{\frac{1}{2}} \exp\left(-\frac{m^*V_{0x}^2}{2kT}\right). \quad (\text{A.3})$$

The velocity v_{0x} is the minimum velocity required in the x-direction to surmount the barrier and is given by the relation

$$\frac{1}{2}m^*V_{0x}^2 = q(V_{bi} - V) \quad (\text{A.4})$$

where V_{bi} and V are the built in potential and the applied voltage respectively (V is positive for forward bias) The electronic concentration n is given by

$$n = N_c \exp\left(-\frac{E_c - E_F}{kt}\right) = 2 \left(\frac{2\pi m^* kT}{h^2}\right)^{\frac{3}{2}} \exp\left(-\frac{qV_n}{kT}\right). \quad (\text{A.5})$$

Substitution of equation (4) and (5) in equation (3) yields

$$J_{s \rightarrow m} = A^* T^2 \exp\left(-\frac{q\phi_{Bn}}{kT}\right) \exp\left(\frac{qV}{kT}\right) \quad (\text{A.6})$$

where

$$A^* = \frac{4\pi q m^* k^2}{h^3}. \quad (\text{A.7})$$

For free electrons $A^* = 120 \frac{\text{amp}}{\text{cm}^2 \text{K}^2} \equiv A$, which is the Richardson constant for Thermionic emission in a vacuum.

Since the barrier height for electrons moving from the metal into the semiconductor remains the same, the current flowing into the semiconductor is thus an affected by the applied voltage. It must therefore be equal to the current flowing from the semiconductor to the metal when thermal equilibrium prevails, i.e., when $V=0$. The corresponding current density is obtained from equation(6) by setting $V=0$

$$J_{s \rightarrow m} = -A^* T^2 \exp\left(-\frac{q\phi_{Bn}}{kT}\right). \quad (\text{A.8})$$

The total current density is given by the sum of equation(6) and equation(8)

$$J_n = \left\{ A^* T^2 \exp\left(-\frac{q\phi_{Bn}}{kT}\right) \right\} \left[\exp\left(\frac{qV}{kT}\right) - 1 \right] \quad (\text{A.9})$$

$$= J_{ST} \left[\exp\left(\frac{qV}{kT}\right) - 1 \right], \quad (\text{A.10})$$

where the saturation current density $J_o = J_{ST}$ is given as

$$J_{ST} = A^* T^2 \exp\left(-\frac{q\phi_{Bn}}{kT}\right). \quad (\text{A.11})$$

Equation A.10 is known as the Thermionic Emission Theory.

Bibliography

- [1] W.Bantikassegn,Phd Dissertation. Electrical property of junction between Aluminium and doped Polyheterocycles.ISBLBN 91-7871-803-1, Linkoping University, Sweden,(1996)
- [2] Alfred Rudin, The Element of Polymer Science and Engineering, Academic Press Inc, London (1982).
- [3] H.Skirakawa, E.J.Louis, A.G MacDiarmid, C.K. Chiang, and A.J. Heeger, J. Chem. Com, **16**(1997)578.
- [4] Prof. Alan J. Heeger, prof. Alan G. MacDiarmid, Prof. Hideki Shirakawa, The Nobel prize in chemistry, 2000: conducting polymers
- [5] Parker IDJ. Appl. Phys.**47**(1994)1656
- [6] J.H. Burroughes,D.D.C Bradley, A.R Brown, R.N. Marks, K. Mackay, R.H Friends, P.L. Burns and A.B. Holmer, Nature, **347**(1990)539.
- [7] Gustafsson G. Caoy, Treasy GM, Klevetter F. Colaneir and Heerer AJ, Nature **357**(1992)477.
- [8] Omheri Y. Manda Y, Takahashi H, Kawai T and Yoshino K. Appl phys. **29**(1990)837
- [9] H.R. Allcock, and F.W. Lampe, Contemporary Polymer Chemistry,^{2nd} edn., Prentice-Hall, New Jersy 1990

- [10] J. Mc Murry, organic chemistry, Books, Monterey, (1984)
- [11] Y. Teketel, PhD, Dissertation, AAU, (1997)
- [12] Yulu, solitons and polarons in conducting polymers, World scientific publishing Co Pte Ltd., (1988)
- [13] Y. Onodara, Phys. Rev., **B30**(1984)775
- [14] G.P. Evens, Advance in Electrochemicals science and Engineering, Vol. 1, VCH Verlagsgesellschaft mbH, (1990)
- [15] S. Roth, One-Dimensional Metal, VCH publishing Inc. New York, NY, (1995)
- [16] N.F. Mott, E.A. Davis, Electronic process in Non Crystalline Materials, 2nded, Oxford, Clarendon Press, (1970)
- [17] T.A Skotheim, R.I. Eisenbuehler and J.R. Reynolds, : hand book of conducting polymer, Marcel Dekker, inc., (1998)
- [18] W. Bantikassegn, O. Inganäs, *Thin solid films*. **293**(1997)138
- [19] M.D. de Leeuw and E.J. Lous, synth. Met, **65**(1994)2511
- [20] G.I. Epifanow, solid state physics, Mir publishers, Moscow, (1979)
- [21] J.R MacDonald, ed., Impedance spectroscopy, Emphasizing solid Materials and system, John Wiley and Sons, New York, (1978)
- [22] E.S Yang, Fundamental of semiconductor Device, McGraw-Hill, Inc., New York, (1992)
- [23] M.S Sze, Physics of semiconductor Device, second ed., John Wiley and Sons, New York, (1981)
- [24] E.H. Rhoderick, and R.H. Williams, Metal-semiconductor contacts, second ed. Oxford University Press, New York, (1988)

[25] G. Girma, Msc. Theses, AAU (1998)

[26] Agilent Technologies Impedance Measurement Handbook December 2003